Holocene hydroclimate changes in continental Croatia recorded in speleothem δ13C and δ18O from Nova Grgosova Cave

Holocene hydroclimate changes in continental Croatia recorded in speleothem $\delta^{13}C$ and $\delta^{18}O$ from Nova Grgosova Cave

Maša Surić[1*], Robert Lončarić[1], Petra Bajo[2], Andrea Columbu[3], Neven Bočić[4], Nina Lončar[1], Russell N. Drysdale[5], John C. Hellstrom[6]

[1] Department of Geography, University of Zadar, Croatia,
[2] Croatian Geological Survey, Zagreb, Croatia
[3] Department of Biological, Geological and Environmental Sciences, Geology Division, University of Bologna, Italy
[4] University of Zagreb, Faculty of Science, Department of Geography, Zagreb, Croatia
[5] School of Geography, The University of Melbourne, Australia
[6] School of Earth Sciences, The University of Melbourne, Australia

Abstract

We present the first stable isotope ($\delta^{13}C$ and $\delta^{18}O$) speleothem record from continental Croatia retrieved from two coeval stalagmites from Nova Grgosova Cave. U-Th dates constrained the growth history from 10 ka to the Recent. We have identified several centennial to millennial-scale hydroclimate oscillations during this period. From 9.2 to 8.8 ka BP the local environmental setting was characterized by enhanced vegetation activity, while during the following 8.2 ka event the main feature was a change in precipitation seasonality. The most prominent change, identified in both $\delta^{13}C$ records, is a sudden decline of vegetation and soil biological activity around 7.4 ka, indicating a decrease in precipitation during the season of maximum plant growth, i.e. dry spring-summer conditions, but most probably also enhanced autumn-winter aridity. Although small in magnitude, the 4.2 ka event (thought to represent a global 'megadrought') was recorded in both the $\delta^{18}O$ and $\delta^{13}C$ time series. Anthropogenic deforestation, which was the first human impact on the environment during the Neolithic agriculture revolution, is excluded as a leading factor in $\delta^{13}C$ variability since the first sedentary settlements were established further to the east in more arable locations along river valleys. However, the impact of intensive mining around the cave site during the last millennium is evident, with substantial deforestation driving an increase in $\delta^{13}C$.

Key words: speleothem, stable isotopes, palaeoclimate, hydroclimate changes, Holocene, Croatia

1. Introduction

Holocene is usually considered to be a warm and relatively stable interglacial compared to the preceding Pleistocene glacial. However, on a finer scale Holocene climate records show numerous temporal and spatial variations (Lowe and Walker, 2015). A comprehensive review using a multiproxy approach by Mayewski et al. (2004) identified six periods of significant rapid climate change during the Holocene: 9.0-8.0 ka, 6.0-5.0 ka, 4.2-3.8 ka, 3.5-2.5 ka, 1.2-1.0 ka and 0.6-0.15 ka BP (where ka BP = 10^3 years before 1950). Wanner et al. (2011) placed several multidecadal to multicentennial cold periods around 8.2 ka, 6.3 ka, 4.7 ka, 2.7 ka, 1.55 ka and 0.55 ka BP. Those events of larger and smaller extent and intensity were driven by different dynamic processes such as low solar activity, ice-sheet meltwater fluxes, fluctuations in North Atlantic overturning circulation, volcanic eruptions and various related feedback effects (Wanner et al., 2011). Other studies have identified single climate anomalies broadly coinciding with quasi-periodic Bond events (Bond et al., 1997; 2001).

Widely recognized Holocene climate events centered on 8.2 and 4.2 ka BP are especially acknowledged in the Global Boundary Stratotype Section and Point (GSSP) tripartite subdivision of the Holocene, with subseries/stage boundaries at 8236 yr b2k (before 2000 CE) and 4250 yr b2k (Walker et al., 2018; Head, 2019). The latter was defined based on the stable isotope profile of the KM-A speleothem from Mawmluh Cave, India (Berkelhammer et al., 2012; Walker et al., 2018), highlighting the importance of speleothem proxy records for palaeoclimate reconstructions and as stratigraphic markers. The number of speleothem-based reconstructions of Holocene environments is increasing worldwide, and of special interest here are those from central and western Europe (Niggemann et al., 2003; Stoykova et al., 2003; Wurth et al., 2004; Genty et al., 2006; Domínguez-Villar et al., 2008; 2009; 2017; Boch et al., 2009; Fohlmeister et al., 2012a; 2012b; Verheyden et al., 2012; Mischel et al., 2017; Allan et al., 2018a; 2018b), eastern Europe (Kacanski et al., 2001; Onac et al., 2002; Tămaş et al., 2005; Constantin et al., 2007; Siklósy et al., 2009; Demény et al., 2013; 2019; Drăguşin et al., 2014) as well as from the Mediterranean region (Bar-Matthews et al., 1999; Zanchetta et al., 2007; 2014; Bar-Matthews and Ayalon, 2011; Zhornyak et al., 2011; Scholz et al., 2012; Regattieri et al., 2014a; 2019; Finne et al., 2014; 2017; Moreno et al., 2017; Psomiadis et al., 2018; Rossi et al., 2018; Budsky et al., 2019; Isola et al., 2019; Baldini et al., 2019).

Here we present the first isotopic research on Croatian continental speleothems, covering the majority of the Holocene using samples recovered from Nova Grgosova Cave (NG hereafter). Previous palaeoenvironmental studies focused on speleothems from submerged and coastal caves (see review in Surić (2018) and references therein) and the aim of this study is to bridge the gap between speleothem records from Adriatic (Rudzka et al., 2012; Lončar et al., 2017; 2019), Alps (Stoykova et al., 2003; Wurth et al., 2004; Mangini et al., 2007; Boch et al., 2009; Fohlmeister et al., 2012a) and Pannonian basin (Siklósy et al., 2009; Demény et al., 2013, Drăguşin et al., 2014) in the context of climate-driven Holocene environmental change. Contemporary monitoring of the Nova Grgosova site has revealed influences of both Mediterranean and Atlantic air masses (Surić et al., 2018), whose relative importance probably shifted during glacial-interglacial cycles, given the location of the cave in south central Europe but only 120 km from the Adriatic Sea.

As previously established, climate reconstructions from a single speleothem could be misleading due to possible site-specific influences (drip hydrology, soil and vegetation cover, cave ventilation etc.) (Fairchild & Baker, 2012; Fohlmeister et al., 2012a). Replicated signals in coeval speleothems from the same cave provide more confidence in palaeoclimate interpretation of isotopic data. Thus, we analyzed two partially coeval speleothems and focused this study on the most pronounced isotopic signals recorded: the 4.2 ka event,

regarded to be a global 'megadrought' (Weiss, 2016), and a potential climate anomaly between 7.5 ka and 7.0 ka BP. Recently, the latter event was hypothesized to be a worldwide multicentennial climate event based on different proxies (lake sediments, ice cores, marine sediments and speleothems), supported by known concurrent social, demographic and cultural transformations (Hou et al. 2019). However, its true global importance remains to be verified, hence local and regional findings such as those presented here can contribute to a better understanding of this proposed climate anomaly during the Holocene Climate Optimum (HCO).

2. Site description

Nova Grgosova Cave (45°49' N; 15°40' E; 239 m a.s.l.) is located in the Samobor hills fluviokarst unit of Žumberačka gora Mountain (NW Croatia) (Fig. 1a). It formed in intensively karstified Neogene lithothamnium limestone (Šikić et al., 1978; 1979; Vrsaljko et al., 2005) and was accidentally exposed in 2004 during quarrying for lime production. Afterwards, the cave atmosphere has been maintained by a well-sealed show-cave steel door. The morphology of the cave is simple – two chambers connected by narrow, partially artificially widened passages, with total length of 97 m (Fig. 1b). Sampling and monitoring have been conducted in the second chamber which is 8 m long, up to 9 m wide, with a minimum height of about 8 m. The overburden above the sampling sites is 5-10 m thick, covered mostly with coniferous forest (Surić et al., 2018). Clastic and mud deposits within the cave point to episodes of fluvial infilling, followed by abundant late Quaternary speleothem deposition (Fig. 1d). Cave position in the epikarst under the hill's summit ensures that the infiltration elevation is just a few dozens of meters above the cave, so neither mixing with groundwater of the phreatic zone nor altitude-modified $\delta^{18}O$ signal significantly impact the dripwater chemistry.

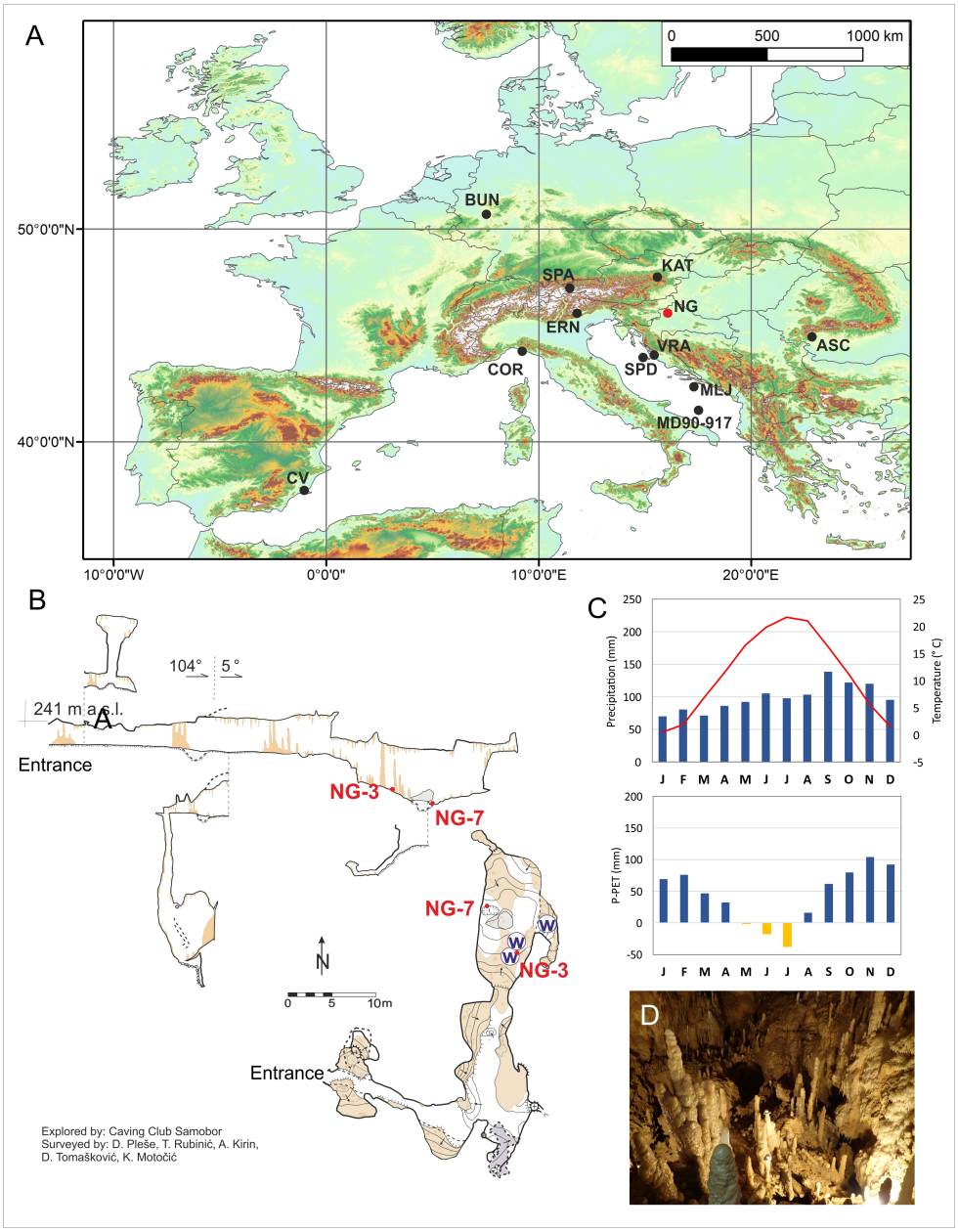

Figure 1 Study site: A) Geographical position of Nova Grgosova Cave (red dot) and other sites used for correlation (black dots): SPA – Spannagel Cave (Fohlmeister et al., 2012a), BUN – Bunker Cave (Fohlmeister et al., 2012b), KAT – Katerloch Cave (Boch et al., 2009), ERN – Grotta di Ernesto Cave (Scholz et al., 2012), COR – Corchia Cave (Zanchetta et al., 2007), CV – Cueva Victoria Cave (Budsky et al., 2019), ASC – Ascunsă (Drăguşin et al., 2014), SPD - Strašna peć Cave on Dugi otok Island (Lončar et al., 2019), MLJ – Mljet Island: Mala špilja Cave (Lončar et al., 2017) and Malo jezero lake sediment (Wunsam et al., 1999), VRA – Vrana lake sediment (Bakrač et al., 2018) and marine core MD 90-917 (Combourieu-Nebout et al., 2013); B) cave survey with marked speleothem (red dots and IDs) and water (W) sampling sites; C) Climate data: average monthly air temperature (station Samobor, 1981-2019), precipitation (station Rude, 1991-2019) and the relation between precipitation and potential evapotranspiration) (CMHS, 2020). Water balance (potential evapotranspiration) is calculated using the Thornthwaite evapotranspiration model (Thornthwaite 1948; McCabe and Markstrom 2007); D) massive speleothem deposition in the chamber where the stalagmites NG-3 and NG-7 were sampled.

The climate of the area corresponds to the Köppen-Geiger Cfb type (temperate humid with warm summers) with a mean annual air temperature (MAAT) of 11.4 °C measured in Samobor (1981-2019) (ca. 3 km to the SE of the cave, elevation ca. 160 m) and average annual precipitation of 1186 mm (1991-2019) measured at the rain gauge station of Rude (ca. 6 km of the cave, elevation ca. 300 m). The highest recorded mean monthly temperature is in July (21.8 °C), and the lowest in January (0.6 °C) (CMHS, 2020) (Fig. 1c). Intra-annual distribution of precipitation is typical for continental Croatia with a peak in September (138.4 mm) reflecting the combined influence of convective and frontal rains during the late summer, and minimum in March (68.5 mm) induced by cold high-pressure continental air masses. Maximum precipitation occurs during the June to September period, but even with enhanced evaporation, aquifer recharge (and in-cave discharge) is present year-round, regardless of the potential evapotranspiration (Fig. 1c).

The stable isotopic composition of the rain and drip water was monitored between November 2014 and October 2015. The local meteoric water line for rainfall was determined to be $\delta^2H = 7.7 \times \delta^{18}O + 12.6$, with a weighted mean *d*-excess of 15.6‰ suggesting both Atlantic and Mediterranean influences (Surić et al., 2020). Drip waters from three sampling sites in the cave showed very good homogenization. Site NG-3 gave $\delta^{18}O$ and δ^2H weighted mean values of -9.8‰ (σ=0.09) and -63.5‰ (σ=0.3) (n = 12), respectively, with no seasonal variations (Surić et al., 2018). The stable isotope composition of drip water reflects the amount-weighted annual mean $\delta^{18}O$ and δ^2H of local precipitation, but the slightly more negative and stable mean value suggests a bias towards winter precipitation, as expected (Surić et al., 2018; 2020).

3. Material and methods

Two candle-shaped stalagmites (NG-3 and NG-7) were taken from the innermost part of the cave (Fig. 1b), both collected in growth position. The 50-cm-long NG-3 was actively growing while the 36-cm-long NG-7 was inactive. Upon collection of NG-3, a drip-logger Stalagmate® (Collister and Mattey, 2005) was installed between November 2014 and November 2017 to measure drip intensity and its relation to rain events. Along with NG-3, two other drip sites (NG-2 and NG-4) were also monitored, all within a few meters of one another, to assess the aquifer architecture. Speleothems were cut longitudinally, then polished to obtain a better insight into the growth layers. The layering in both stalagmites is similar in shape and diameter, whilst the petrography is very homogenous with the exception of the youngest part of NG-3, which is the most translucent section. Neither dissolutional nor diagenetic macro-scale alteration is evident in polished section, and the absence of dissolution cups along the central axes suggests that drip waters have never been undersaturated with respect to calcite.

Samples for stable isotope analyses were drilled at 1 mm increments along the growth axes using a tungsten carbide 1-mm dental drill attached to a computer-controlled Taig CNC micromilling lathe. In addition, samples along 6 single laminae of each speleothem were taken for the purpose of Handy tests (Hendy, 1971). A total of 909 $\delta^{18}O$ and $\delta^{13}C$ analyses were performed by AP2003 continuous-flow isotope-ratio mass spectrometry at the School of Geography, The University of Melbourne, following the same protocol as described in Bajo et al. (2020). Results are expressed in the delta notation relative to the Vienna Pee Dee Belemnite (V-PDB) international scale. Sample results were normalized using internal NEW-1 and NEW-12 standards and the international standard reference material, NBS-19. Analytical uncertainty for $\delta^{18}O$ and $\delta^{13}C$ were better than 0.01‰ and 0.05‰, respectively.

U-Th ages were derived from 28 solid calcite prisms (51-200 mg) extracted along the growth axes. Chemical preparation followed the method of Hellstrom (2003). Isotopic

measurements were performed by a Nu Instruments Plasma MC-ICPMS at the School of Earth Sciences, University of Melbourne, following the procedure described in Hellstrom (2003). The initial $^{230}Th/^{232}Th$ activity ratio was constrained to 2.70 ± 0.65 by using a Monte-Carlo-based Finite Positive Growth Rate Model approach (Hellstrom 2006; Corrick et al., 2020). In this age-depth modelling approach sample age and depth together with their uncertainties are used as input parameters. For each of 10 000 iterations performed, age and depth for each sample are randomized taking into account their uncertainties, then sorted by their randomized depths. A least-squares procedure is then used to find the sequence of connecting positive growth rate age-depth line segments which best fit the uncertainty-weighted age-depth data. Finally, the 3rd-, 50th- and 97th-percentile interpolated ages were determined at 500 evenly-spaced steps along the depth profile. Final isotopic time series were obtained by interpolating the age-depth model data onto the stable isotope depth profiles of the two speleothems.

4. Results

4.1. Monitoring

Reliable interpretation of speleothem proxy records partly relies on characterisation of the processes operating in the overlying karst aquifer (Baker et al., 1997a; Baldini et al., 2006). After the 3-year monitoring of three closely spaced drip sites, it is evident that the aquifer is characterized by triple (conduits, fracture and matrix) porosity (White, 1999; Fairchild and Baker, 2012) which results with quite different discharge features in spite of the proximity of the drips (Fig. 2). Unlike variable drip rates of the adjacent NG-2 and NG-4 sites (described in Surić et al. (2018)), drip site NG-3 was practically unresponsive to surface events, maintaining a typical 12-13 drips/hour regardless of the rainfall intensities and amounts. According to the classification of the groundwater flow types based on the relationship between mean discharge and discharge variability (after Smart and Friederich, 1987 and Baker et al., 1997a), the NG-3 drip site belongs to the 'seepage-flow' class. Therefore, the aforementioned drip water homogenization (Surić et al., 2018) indicates that the isotopic signal transferred to the spelean calcite is most sensitive to long-term (i.e. decadal or longer) environmental changes.

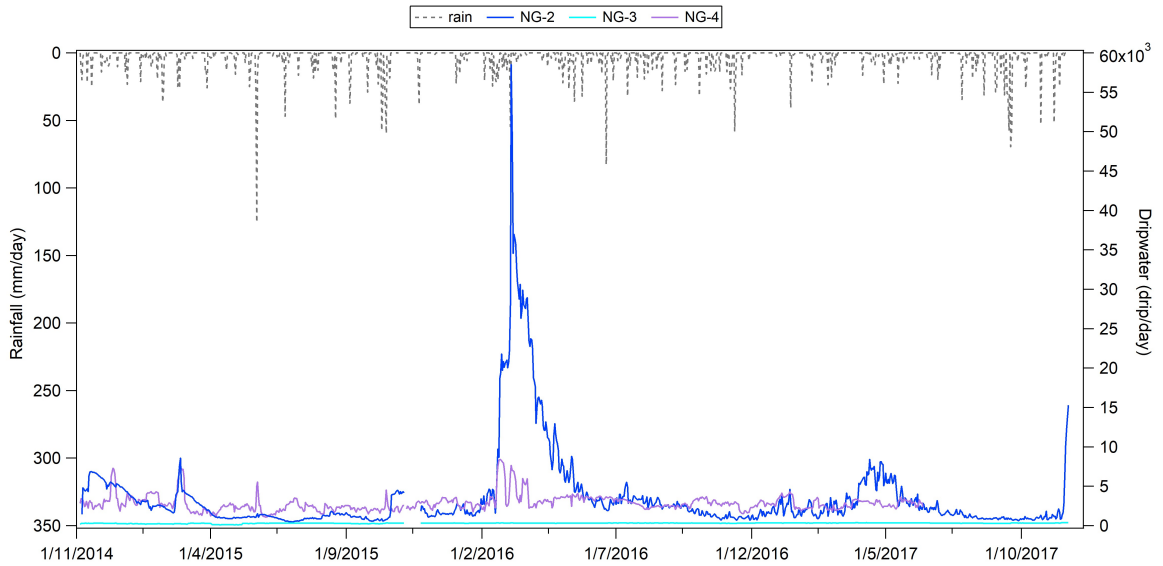

Figure 2 Response of the drip sites to the rain events from November 2014 to October 2017. Daily precipitation data are from the adjacent meteorological stations Rude (6 km from Nova Grgosova Cave)

4.2 Chronology

U-Th dating results are presented in Table 1. Average ^{238}U concentration in both stalagmites was 362 ppb (227-456 ppb). Detrital contamination, expressed by the $^{230}Th/^{232}Th$ activity, ranged from 5.3 to 648.3. Therefore, correction for detrital Th content was applied using initial activity ratios of detrital thorium $(^{230}Th/^{232}Th)_i$ of 2.70 ± 0.65 (Hellstrom, 2006). All ages are in stratigraphic order within 2σ uncertainty; this is a further evidence of the absence of diagenetic phenomena at even the micro-scale, which would have caused modifications in the original U-Th geochemical system, resulting in age inversions or outliers (Bajo et al., 2016). According to the U-Th age models (Fig. 3), NG-3 grew continuously throughout the Holocene from $10.09^{+0.25}/_{-0.17}$ ka) until the date of sampling. NG-7 stalagmite overlaps with NG-3 for the period $7.89^{+0.57}/_{-0.22}$ ka to $5.70^{+0.11}/_{-0.12}$ ka (Fig. 4). Stalagmite NG-7 showed relatively uniform growth (Fig. 5), with an average rate of 164 mm/ka, while NG-3 grew generally slower with average rate of 50 mm/ka. The slowest NG-3 growth phases were from $5.57^{+0.08}/_{-0.22}$ ka to $4.17^{+0.25}/_{-0.07}$ ka, and between $2.64^{+0.14}/_{-0.33}$ ka and $0.11^{+0.12}/_{-0.05}$ ka with 29.9 and 20.1 mm/ka, respectively. An increased growth rate of 110.5 mm/ka occurred between $4.12^{+0.05}/_{-0.05}$ ka and $3.83^{+0.07}/_{-0.06}$ ka (Fig. 5).

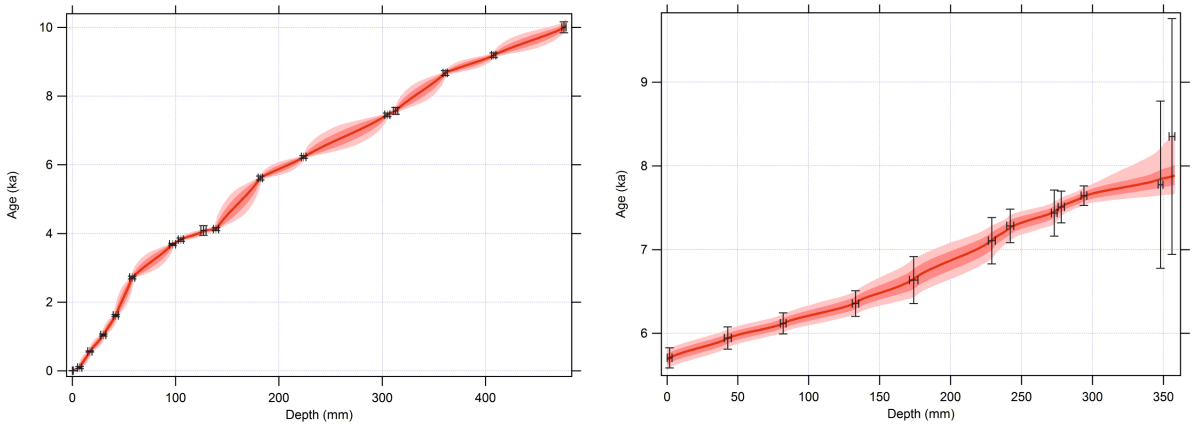

Figure 3 Age-depth models for NG-3 and NG-7. The outer shaded zone defines the 95% confidence interval.

Table 1 Corrected U-Th ages for NG-3 and NG-7 speleothems. The activity ratios have been determined after Hellstrom (2003). Ages are calculated using the decay constant of Cheng et al. (2013) and initial $^{230}Th/^{232}Th$ of 2.70 ± 0.65 (Hellstrom, 2006).

Sample ID	Mass (g)	^{238}U (ng/g)	Depth (mm from top)	$(^{230}Th/^{238}U)_A$	2σ	$(^{234}U/^{238}U)_A$	2σ	Uncorrected age (ka)	2σ	$(^{232}Th/^{238}U)_A$	2σ	$(^{230}Th/^{232}Th)_A$	Corrected age (ka)	2σ	$(^{234}U/^{238}U)_{In}$	2σ
NG3-2	0.0790	334	7 ± 2.00	0.0019	0.0002	1.0624	0.0036	0.195	0.021	0.000362	0.000002	5.3	0.095	0.032	1.0624	0.0036
NG3-12	0.1640	411	17 ± 2.00	0.0061	0.0001	1.0772	0.0022	0.619	0.010	0.000203	0.000002	30.0	0.564	0.017	1.0773	0.0022
NG3-16	0.0920	421	30 ± 2.50	0.0112	0.0003	1.1203	0.0012	1.095	0.029	0.000205	0.000002	54.5	1.042	0.032	1.1207	0.0012
NG3-15	0.0810	277	42 ± 2.50	0.0175	0.0003	1.1581	0.0009	1.660	0.028	0.000193	0.000004	90.2	1.611	0.031	1.1588	0.0009
NG3-11	0.1240	279	58 ± 2.50	0.0292	0.0003	1.1378	0.0021	2.834	0.030	0.000447	0.000007	65.4	2.717	0.041	1.1389	0.0021
NG3-10	0.2000	361	97 ± 3.00	0.0390	0.0002	1.1421	0.0025	3.786	0.021	0.000395	0.000007	98.9	3.684	0.033	1.1436	0.0025
NG3-9	0.1450	456	105 ± 2.50	0.0374	0.0004	1.0625	0.0019	3.906	0.043	0.000316	0.000009	118.1	3.819	0.048	1.0632	0.0019
NG3-8	0.1900	446	127 ± 2.50	0.0453	0.0007	1.0996	0.0025	4.585	0.073	0.001851	0.000064	24.5	4.089	0.140	1.1008	0.0026
NG3-7	0.1830	410	139 ± 2.50	0.0454	0.0004	1.1922	0.0021	4.229	0.039	0.000419	0.000009	108.3	4.126	0.045	1.1944	0.0021
NG3-14	0.0560	371	182 ± 2.00	0.0616	0.0006	1.2210	0.0015	5.637	0.057	0.000095	0.000002	648.3	5.614	0.057	1.2245	0.0015
NG3-6	0.1780	287	224 ± 2.25	0.0697	0.0004	1.2480	0.0023	6.255	0.039	0.000126	0.000002	554.3	6.226	0.039	1.2524	0.0023
NG3-5	0.1980	353	305 ± 2.50	0.0809	0.0005	1.2084	0.0021	7.542	0.050	0.000367	0.000009	220.4	7.453	0.054	1.2128	0.0021
NG3-4	0.1350	362	313 ± 2.00	0.0863	0.0007	1.2398	0.0022	7.850	0.067	0.001197	0.000004	72.1	7.568	0.096	1.2450	0.0022
NG3-13	0.0900	348	365 ± 2.00	0.0996	0.0007	1.2862	0.0012	8.765	0.065	0.000413	0.000007	241.4	8.670	0.069	1.2933	0.0012
NG3-3	0.0910	325	412 ± 2.00	0.1100	0.0007	1.3444	0.0023	9.276	0.064	0.000398	0.000005	276.4	9.190	0.067	1.3534	0.0023
NG3-1	0.0510	353	480 ± 2.00	0.1224	0.0018	1.3757	0.0049	10.120	0.162	0.000547	0.000006	223.9	10.003	0.161	1.3865	0.0050
NG7-2	0.0523	329	2 ± 1.75	0.0558	0.0009	1.0471	0.0039	5.969	0.101	0.000931	0.000005	60.0	5.707	0.120	1.0479	0.0040
NG7-11	0.1560	402	43 ± 2.50	0.0575	0.0011	1.0465	0.0016	6.160	0.121	0.000775	0.000003	74.2	5.943	0.133	1.0473	0.0016
NG7-10	0.1780	435	82 ± 2.00	0.0604	0.0008	1.0470	0.0020	6.476	0.090	0.001272	0.000006	47.5	6.118	0.125	1.0478	0.0020
NG7-9	0.1140	405	133 ± 2.25	0.0629	0.0011	1.0517	0.0022	6.722	0.122	0.001304	0.000006	48.3	6.356	0.153	1.0526	0.0022
NG7-8	0.1860	342	174 ± 3.00	0.0727	0.0006	1.0582	0.0018	7.757	0.067	0.004014	0.000017	18.1	6.637	0.281	1.0593	0.0018
NG7-7	0.0990	327	229 ± 2.50	0.0778	0.0005	1.0699	0.0018	8.226	0.057	0.004047	0.000073	19.2	7.107	0.278	1.0713	0.0018
NG7-6	0.1860	298	242 ± 2.50	0.0764	0.0007	1.0727	0.0023	8.050	0.080	0.002793	0.000007	27.4	7.283	0.200	1.0742	0.0023
NG7-5	0.1000	317	277 ± 2.00	0.0805	0.0011	1.0793	0.0020	8.445	0.122	0.003685	0.000009	21.8	7.437	0.275	1.0810	0.0021
NG7-4	0.1040	392	282 ± 2.25	0.0785	0.0007	1.0789	0.0020	8.230	0.077	0.002634	0.000034	29.8	7.510	0.190	1.0806	0.0020
NG7-3	0.1370	434	298 ± 2.00	0.0771	0.0005	1.0799	0.0020	8.070	0.056	0.001564	0.000029	49.3	7.644	0.116	1.0816	0.0020
NG7-1	0.0501	318	352 ± 1.75	0.1123	0.0011	1.0974	0.0038	11.754	0.129	0.014611	0.000035	7.7	7.776	0.999	1.0995	0.0039
NG7-12	0.0530	339	360 ± 2.00	0.1331	0.0012	1.1082	0.0015	13.925	0.137	0.020462	0.000500	6.5	8.351	1.410	1.1108	0.0016

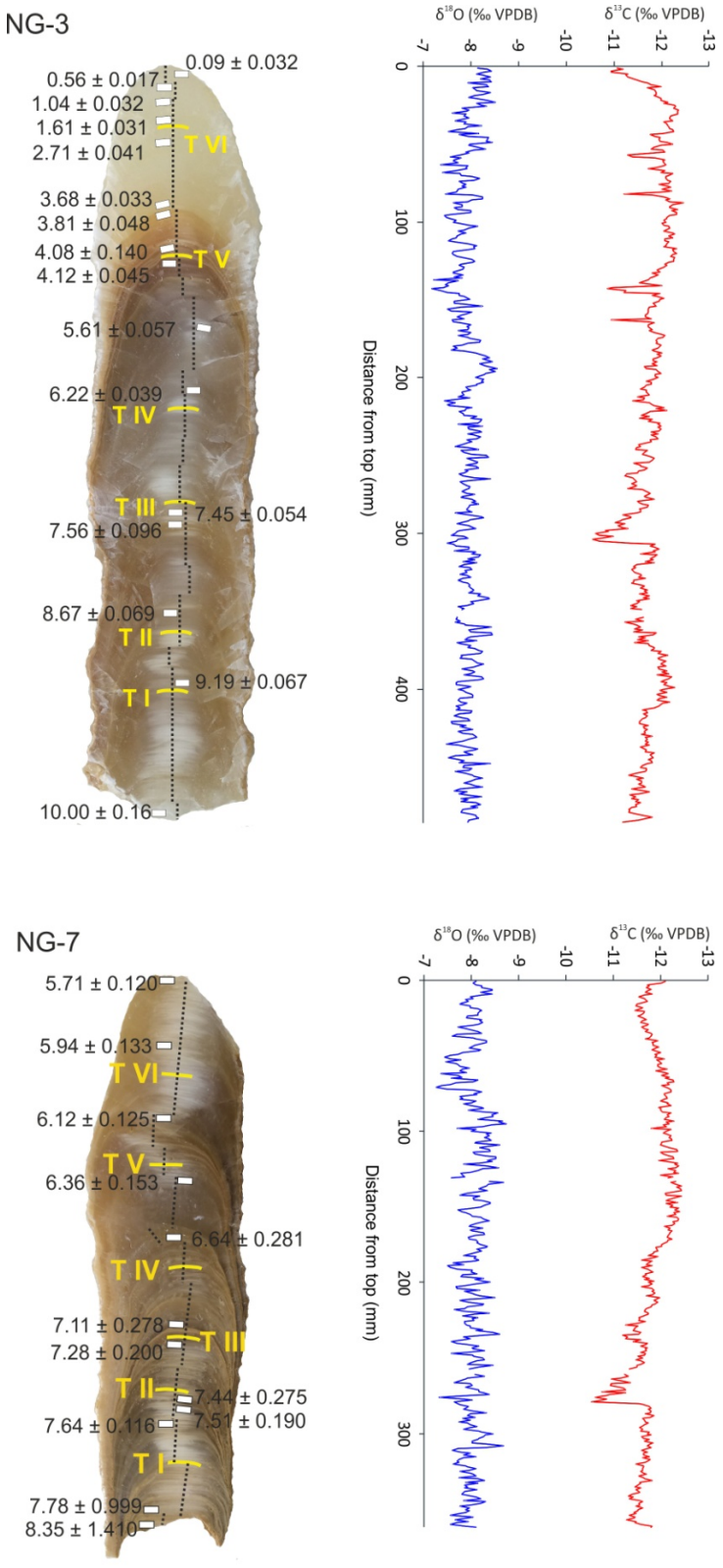

Figure 4. NG-3 and NG-7 stalagmites with marked sampling positions and plots of stable isotope composition against depth. White rectangles mark the positions of dated samples with U-Th ages ± 2σ uncertainties given in ka. Stable isotope sampling transects are marked with black dotted lines, while yellow lines represent laminae where Hendy tests (Hendy, 1971) were performed. Stable isotope samples from 350-353 mm in NG-3 and 258-260 mm in NG-7 are missing due to the stalagmite breakages during transport.

4.3 Stable isotopes

The $\delta^{13}C$ and $\delta^{18}O$ variations recorded along the growth axes of NG-3 and NG-7 stalagmites vs. depth and vs. age are shown in Figures 4 and 5, respectively. NG-3 has a mean $\delta^{18}O$ value of -7.94‰ (range from -8.56‰ to -7.19‰) and mean $\delta^{13}C$ of -11.76‰ (range from -12.45‰ to -10.57‰). In NG-7, the mean $\delta^{18}O$ value is -8.03‰ (range from -8.73‰ to -7.25‰) and the mean $\delta^{13}C$ is -11.81‰ (range from -12.44‰ to -10.53‰). The average temporal resolution of the stable isotope data based on the U-Th age models is 21 yr (from 4.4 yr to 74 yr) for NG-3, and 6.1 yr (from 2.8 yr to 15.2 yr) for NG-7 stalagmite. The $\delta^{18}O$ in NG-3 was relatively invariant, with an amplitude of <1.4‰ (Fig. 4), and with the highest value centred at 4.29 ka (Fig. 5). In NG-7, $\delta^{18}O$ was also relatively stable, varying within <1.2‰, (Fig. 4). As for the $\delta^{13}C$ variations, they are more pronounced and generally do not co-vary with $\delta^{18}O$ in either speleothem. The most prominent $\delta^{13}C$ signal, clearly recorded in both speleothems, is a positive shift around 7.4-7.5 ka (Fig. 5).

Confident hydroclimate interpretation of stable isotope records is acceptable in cases where near-equilibrium isotopic fractionation during calcite precipitation from the drip water can be demonstrated (Hendy, 1971, McDermott, 2004). In the NG speleothems this was confirmed using three approaches (Supplementary material). Firstly, Hendy test (Hendy, 1971) results suggest that deposition of both speleothems did not occur in isotopic disequilibrium (Figs. S1, S2, S3). This is verified by the replication test (Dorale and Liu, 2009) between overlapping NG-3 and NG-7 sections (Fig. S4). Finally, this conclusion is supported by comparison of measured cave air temperature (11.4 °C) with that calculated (10.8±0.4 °C) from the uppermost calcite of NG-3 according to empirical relationships for water-calcite oxygen isotope fractionation proposed by Tremaine et al. (2011). The latter is used with the presumption that if modern spelean calcite confirms equilibrium conditions, then ancient speleothems from the same cave environment should also have been precipitated at or near isotopic equilibrium (Mickler et al., 2004).

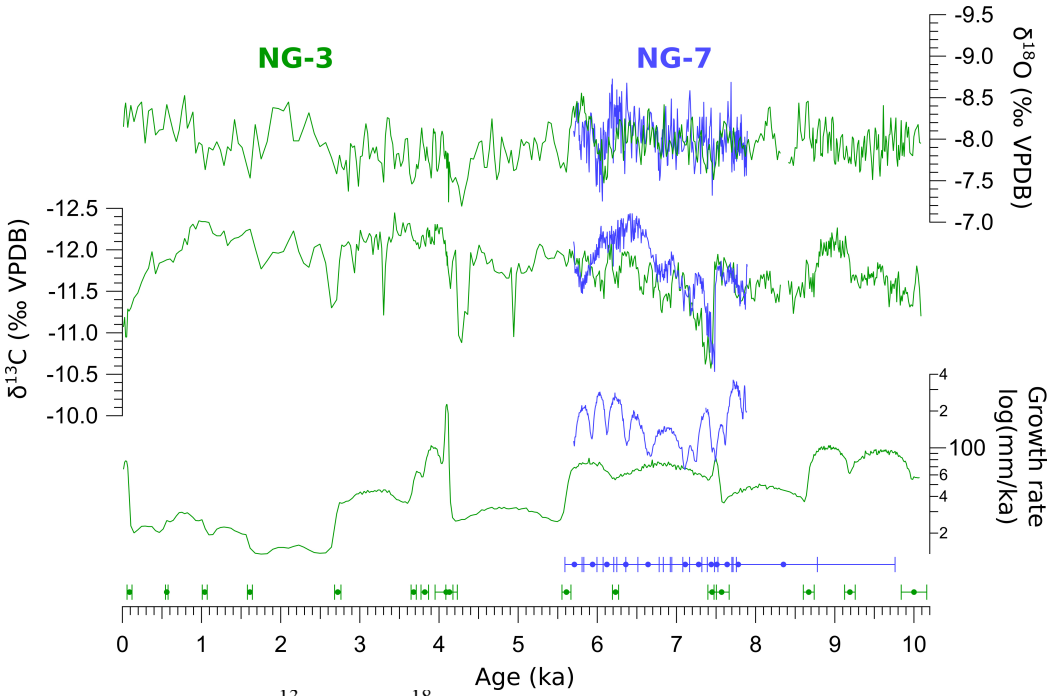

Figure 5 Comparison of $\delta^{13}C$ and $\delta^{18}O$ time series and growth rates of NG-3 and NG-7 speleothems. Dots represent U-Th ages with the 2σ-error bars used for the age model of NG-3 and NG-7, respectively.

5. Discussion

5.1 $\delta^{18}O$ and $\delta^{13}C$ interpretation

At orbital time scales, oxygen stable isotope ($\delta^{18}O$) records in stalagmites demonstrate palaeoenvironmental changes generally related to global climate changes, but at shorter timescales the response to climatic conditions can also be influenced by regional and/or local/site-specific factors (McDermott et al., 2011). Provided that near-equilibrium calcite deposition has occurred, spelean $\delta^{18}O$ is influenced by both cave air temperature and dripwater $\delta^{18}O$ values (Hendy, 1971), which in turn depends on meteoric water $\delta^{18}O$ values and potential influences regarding latitude, altitude, continentality, air temperature and rainfall amount (Rozanski et al., 1982; 1993), along with processes within the soil, epikarst and the drip site in the cave (Fairchild and Baker, 2012). Numerous speleothem-based studies have revealed predominant influences, usually temperature or rainfall amount effect, in various regions, but not yet in continental Croatia. In the Mediterranean basin, for example, $\delta^{18}O$ is mainly influenced by the precipitation amount effect which leads to more negative (positive) speleothem $\delta^{18}O$ values during the humid (dry) interglacial and interstadials (glacial and stadials) periods due to $\delta^{18}O$-depleted (enriched) precipitation. It has been shown from north and central Italy (e.g. in Corchia Cave by Zanchetta et al. (2007), Drysdale et al. (2009), Regattieri et al. (2014a); in Tana che Urla Cave by Regattieri et al. (2014b); in Renella Cave by Zhornyak et al. (2011); in Rio Martino Cave by Regattieri et al. (2019)), in southern Italy (e.g Pozzo Cucú Cave by Columbu et al. (2020)), in Sardinia (e.g. Bue Marino and Crovassa Azzurra Caves by Columbu et al. 2017, 2019); then in Kapsia Cave (Finné et al., 2014) and Skala Marion Cave (Psomiadis et al., 2018) in Greece, in Soreq and Peqiin caves in Israel (e.g. Bar-Matthews et al., 2003) and in littoral Croatia in Modrič Cave (Rudzka et al., 2012) Strašna peć Cave (Lončar et al., 2019) and Mala špilja and Velika špilja caves (Lončar et al., 2017). A similar response is recorded also further to the east, e.g. in North Macedonian Lake Ohrid Cave (Regattieri et al., 2018), Dim Cave in Turkey (Ünal-İmer et al., 2015) or Iranian Qal'e Kord Cave (Mehterian et al., 2017), as well as in French Villars Cave (Genty et al., 2003; 2006) and Bourgeois-Delaunay Cave (Couchoud et al., 2009), and the Iberian Buraca Gloriosa Cave (Thatcher et al., 2020). In addition, the same isotopic effects are reported in the southern Alps (Frisia et al., 2005; Belli et al., 2013; Columbu et al., 2018), but also in Austrian Alps in Spannagel Cave (Mangini et al., 2007; Fohlmeister et al., 2012a).

On the other side, in continental ('non-Mediterranean') West and Central European sites west of NG cave, the $\delta^{18}O$ response to climate variations is governed by the temperature effect, producing isotopic values that shift in the same direction as those in Greenland ice cores (NGRIP project members, 2004), with lower $\delta^{18}O$ values associated with low temperatures during colder periods, and vice versa, as reported from the north Alps speleothems (e.g. Spötl et al., 2002; 2006; 2008; Boch et al., 2009; 2011; Moseley et al., 2015; 2020). The same pattern is recorded in Crag Cave in SW Ireland (McDermott et al., 2001), Hüttenbläserschachthöhle Cave in Germany (Scholz et al., 2019), in Kaite Cave (Domínguez-Villar et al., 2008) and La Garma Cave in northern Spain (Baldini et al., 2019). Temperature controlled $\delta^{18}O$ is also revealed in modern speleothem from Postojna Cave in Slovenia (Domínguez-Villar et al., 2018).

To the east and northeast of our study site, in the Pannonian basin and Carpathian region, $\delta^{18}O$ also decreases during the glacial stages, as reported in Hungarian Abaliget Cave (Koltai et al., 2017), Baradla Cave (Demény et al., 2017) and Leány Cave (Demény et al., 2013). In western Romanian caves Ascunsă (Drăguşin et al., 2014), Poleva (Constantin et al., 2007) and Urşilor Cave (Onac et al., 2002) Holocene $\delta^{18}O$ variations generally reflect temperature changes (Drăguşin et al., 2014). In Sofular and Ovacik caves in Turkey, isotopic

changes reflect temperature and moisture source effect changes related to the Black Sea (Fleitmann et al., 2009; Göktürk et al., 2011). In terms of dominant effects, such simplified regional delimitations can conceal other local drivers that interrupt the primary signal, e.g. changes in the proportions of winter and summer precipitation (Mangini et al., 2005), influence of the local topography on cyclogenesis and thermal depressions (Trigo et al., 2002) or switches in the main precipitation sources (Lüetscher et al., 2015).

Based on the 43-year-long precipitation record from Zagreb (24 km east of Nova Grgosova Cave) (Krajcar Bronić et al., 2020), as well as our 1-year observations at the cave site (Surić et al., 2018), no significant correlation is found between monthly $\delta^{18}O$ and precipitation amount as the latter evidently shows a lack of seasonality. The observed temperature gradient of rainwater $\delta^{18}O$ in Zagreb is 0.331±0.013 ‰/°C (n=394; r=0.80) (Krajcar Bronić et al., 2020) which leads to isotopic enrichment with temperature increase. At the same time, temperature dependent calcite-water oxygen isotope fractionation has a gradient of -0.24‰/°C (Kim and O'Neil, 1997), or more recently proposed -0.18‰/°C (Tremaine et al., 2011), so the net dependence of calcite $\delta^{18}O$ on formation temperature is between 0.16 and 0.08‰/°C, depending on the water-calcite fractionation coefficient used. So, even the minimal $\delta^{18}O$ variations in NG speleothems throughout Holocene would have required unrealistically large temperature variations (e.g. overall, the NG-3 Holocene $\delta^{18}O$ amplitude of 1.37‰ would require a temperature shift of 9-17 °C). Accordingly, it is more likely that $\delta^{18}O$ is a hydrological proxy related to vapour source and/or multiannual rainfall amount changes, as generally recognized and applied within the Mediterranean region. Given the bordering position of Nova Grgosova Cave region within central Europe, it is likely that during glacial-interglacial transitions the alteration of vapour sources might have occurred, as well as shifts in dominant effects – source, amount and/or temperature, as recorded northern, western and eastern from our site.

Along with $\delta^{18}O$, the most frequently used speleothem proxy is $\delta^{13}C$, whose variations reflect the environmental changes in several ways. First-order changes are often due to climate-driven vegetation change manifested as alteration of C3 and C4 dominated plant assemblages above the cave. Given the geographical position of Nova Grgosova Cave in the temperate zone, this cause is unlikely as the region is characterized solely by C3 vegetation with typical mid-latitude speleothem $\delta^{13}C$ values ranging from -14‰ to -6‰ (McDermott, 2004). As demonstrated in several studies (e.g. Drysdale et al., 2004; Frisia et al. 2005; Scholz et al., 2012; Zanchetta et al., 2007; Rudzka et al., 2012; Belli et al., 2013; Regattieri et al., 2014b; 2018; Koltai et al., 2017; Lončar et al., 2017; Demény et al., 2019; Columbu et al., 2020) the dominant influence in nearby locations at comparable latitude is vegetation and soil microbial activity. Indeed, this is expressed with lower speleothem $\delta^{13}C$ values resulting from higher pCO_2 in the soil, due to denser and more productive vegetation and root respiration during wetter periods, and higher $\delta^{13}C$ values during dry periods and reduced bio-pedological activity. Furthermore, decreased precipitation and consequent reduced aquifer recharge result in slower flow rates and prolonged rock-water interaction, leading to higher contribution of hostrock-derived carbon (Baker et al., 1997b) and enhanced prior calcite precipitation (PCP) (Fairchild et al., 2000; McDermott, 2004). Both these processes cause higher dripwater and subsequent speleothem $\delta^{13}C$ values (Bajo et al., 2017).

Given the uniform annual precipitation distribution (Fig. 1c), year-round stable drip rates (Fig. 2), thorough homogenization of the rainwater within the aquifer (Surić et al., 2018) and near-equilibrium calcite precipitation confirmed by replicated $\delta^{13}C$ signals in both NG speleothems, we can regard $\delta^{18}O$ and $\delta^{13}C$ as reliable proxies for multi-annual climate-driven changes of local environment. Since microbial activity in the soil and vegetation density above the cave is at its highest during spring/summer season the $\delta^{13}C$ is most likely a proxy for spring/summer environmental conditions. Furthermore, cave monitoring data point to the

autumn/winter as main recharge season and we interpret $\delta^{18}O$ as a proxy for predominantly autumn/winter conditions.

5.2. Lower (Early) Holocene

The Greenlandian stage (i.e. Lower/Early Holocene: 11.6-8.2 ka) is recorded in NG-3 speleothem only from ~10.1 ka onwards. The $\delta^{18}O$ and $\delta^{13}C$ variability in the NG record is minimal, ranging between -8.46‰ and -7.51‰ and from -12.27‰ to -11.20‰, respectively. The only noticeable shift is a $\delta^{13}C$ decrease and its apparent stability between 9.2 ka and 8.8 ka (Fig. 5). Similar excursions that could point to more favourable conditions for vegetation above the cave, to our knowledge, has not been registered in nearby speleothem records or other proxies, except as an abrupt and rather short-lived negative $\delta^{18}O$ shift at $9.15^{+0.06}/_{-0.06}$ ka in Spannagel Cave (Fohlmeister et al., 2012a) and at 8.91 ka in Bunker Cave (Fohlmeister et al., 2012b) in otherwise quite variable parts of these records (Fig. 6). Climate anomalies recorded by $\delta^{18}O$ decrease around 9 ka in northern Iberia La Garma Cave (Baldini et al., 2019), Herbstlabyrinth Cave at $9.1^{+0.20}/_{-0.20}$ ka (Mischel et al., 2017) and in Alpine Katerloch Cave (Boch et al., 2009) are associated with the '9.2 ka event' which was detected in numerous climate proxies in Northern Hemisphere (Fleitmann et al., 2008 and references therein) and was ascribed as a response to one of several meltwater pulses (MWP) that preceded the major outburst at 8.2 ka. On the Mediterranean side, the Mean Anomaly Index (MAI) derived from the combined $\delta^{18}O$, $\delta^{13}C$ and Mg/Ca time series from Corchia Cave (Regattieri et al., 2014a) points to longer dry period between ca. 9.2 ka and 8.4 ka interrupted by one brief wet episode centred at 8.6 ka (Fig. 7). However, it does not correlate with the wet episode at Nova Grgosova Cave site within the corresponding age uncertainties, although subsequent dry and wet episodes demonstrated relatively good matching of these two records. East of Nova Grgosova Cave, in Romanian cave V11, short negative $\delta^{18}O$ shifts are recorded at 9.3 ka (Tămaş et al., 2005) and at 9.2 ka in Poleva Cave (Constantin et al., 2007), but both are brief cold episodes. Notwithstanding this, the 400-year period of lower $\delta^{13}C$ in NG-3, associated with decreasing $\delta^{18}O$ and increasing growth rate, suggests the environmental conditions improved in terms of vegetation cover. However, without replication or other regional records, we tentatively ascribe this multi-centennial episode to local background hydroclimate variability for the time.

Following this negative shift, the $\delta^{13}C$ shows a trend of increasing values for the next ~600 years, towards '8.2 ka event'. That short-lived near-global phenomenon of North Atlantic cooling was likely caused by an abrupt outburst of North American proglacial lakes Agassiz and Ojibway at ~8.47 ka (Lajeunesse and St-Onge, 2008). It triggered a reduction in the Atlantic Meridional Overturning Circulation (AMOC), a $\delta^{18}O$ depletion of subpolar North Atlantic surface ocean water and a climate anomaly across Europe, as documented in various archives including speleothems. However, its registration in speleothems is inconsistent (Lechleitner et al., 2018). For example, whilst it has been detected in south Belgian stalagmites from Père Noël Cave (Allan et al., 2018b), in Herbstlabyrinth cave system, Central Germany (Mischel et al., 2017), in Austrian Katerloch Cave (Boch et al., 2009), and in Kaite Cave in north Spain (Domínguez-Villar et al., 2009), it did not produce an unequivocal isotopic signature in Spanish El Soplao Cave (Rossi et al., 2018). Similarly, the 8.2 ka anomaly is not recorded in Romanian caves Poleva (Constantin et al., 2007) and V11 (Tămaş et al., 2005), although it is clearly identifiable in other regional records (peat bog pollen, lacustrine, marine sediments). In Ascunsă Cave, the 8.2 ka event is recorded only by higher growth rate (Drăguşin et al., 2014). In our NG record, an increase of $\delta^{18}O$ is apparent between $8.54^{+0.11}/_{-0.27}$ ka to $8.18^{+0.29}/_{-0.34}$ ka, but the full amplitude of isotopic variability during this time is unknown due to the 4 mm of missing calcite at the point where the speleothem fractured (equivalent to ~4 missing samples, and spanning several 100(s) years)

(Fig. 6a). Based on the significantly lower $\delta^{13}C$ variability over the same period, we can assume that water availability was only perhaps slightly disturbed at most, as notable in partly decreased growth rate (Fig 5). Increased $\delta^{18}O$ values might thus reflect a decrease in lower $\delta^{18}O$ autumn-winter rainwater, suggesting a change in precipitation seasonality. Temperature shifts cannot be resolved, although they were estimated down to -3 °C in Austria's Katerloch Cave (Boch et al., 2009).

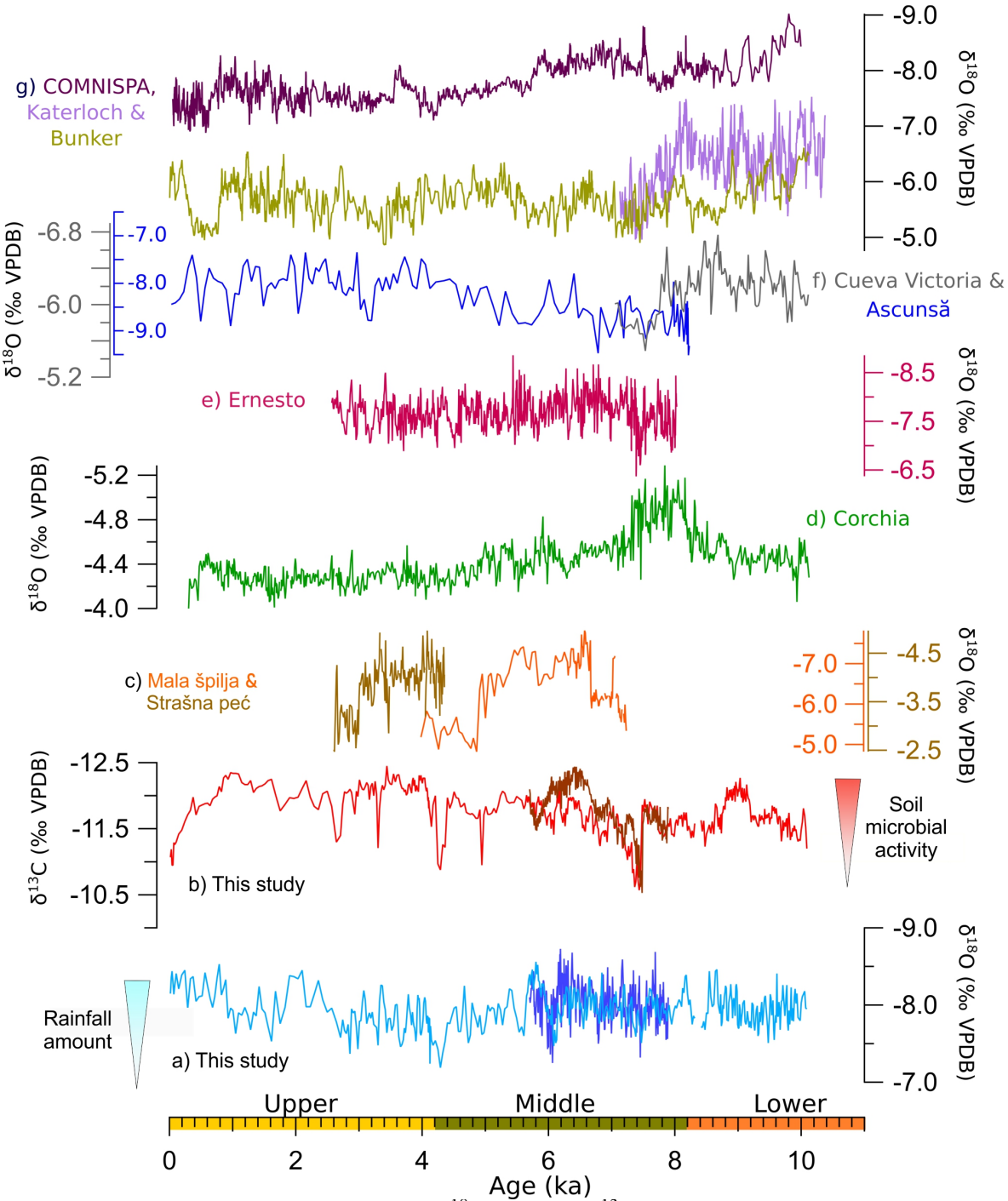

Figure 6. NG-3 and NG-7 stalagmites $\delta^{18}O$ (a) and $\delta^{13}C$ (b) time series compared to other speleothem data from: c) Mala špilja Cave (Lončar et al., 2017) and Strašna peć Cave (Lončar et al., 2019); d) Corchia Cave (Zanchetta et al., 2007; Bajo et al., 2016); e) Ernesto Cave (Scholz et al., 2012); f) Ascunsă Cave (Drăguşin et al., 2014) and Cueva Victoria

(Budsky et al., 2019); g) Spannagel Cave (Fohlmeister et al., 2012a), Katerloch Cave (Boch et al., 2009) and Bunker Cave (Fohlmeister et al., 2012b).

5.3. Middle Holocene

Northgrippian stage (i.e. Middle Holocene: 8.2-4.2 ka) changes were captured in both NG speleothems. The most prominent and abrupt increase of $\delta^{13}C$ values was recorded at ~7.4 ka ($7.43^{+0.07}/_{-0.11}$ ka in NG-3 and $7.48^{+0.10}/_{-0.13}$ ka in NG-7), potentially corresponding to Bond event 5 (Bond et al., 2001). High correlation between $\delta^{13}C$ values of NG-3 and NG-7 speleothems strongly suggest the signal reflects at least local climate conditions, rather than site-specific effects. Moreover, similar positive, usually short-lived, excursions have been reported in several other European speleothem $\delta^{18}O$ records, with almost the same timing: in Spannagel Cave at $7.45^{+0.02}/_{-0.03}$ ka (Fohlmeister et al., 2012a), Bunker Cave at $7.45^{+0.41}/_{-0.28}$ ka (Fohlmeister et al., 2012b), Ernesto Cave at $7.45^{+0.44}/_{-0.44}$ ka (Scholz et al., 2012), Corchia Cave at $7.46^{+0.09}/_{-0.08}$ ka (Zanchetta et al., 2007) and in Cueva Victoria at $7.53^{+0.37}/_{-0.28}$ ka (Budsky et al., 2019) (Fig 6) indicating a climate event with regional impact. Elevated speleothem $\delta^{18}O$ values from Mala špilja Cave (Mljet Island, SE Adriatic) are centred to $7.23^{+0.10}/_{-0.10}$ ka (Lončar et al., 2017). All these sites are characterized by increased speleothem $\delta^{18}O$ values during cold and dry periods, even those short-lasting, thus we suggest that such an event around 7.4-7.5 ka decreased biological activity above Nova Grgosova Cave and/or prolonged residence time of groundwater in the aquifer, both leading to a $\delta^{13}C$ increase. A positive $\delta^{13}C$ shift is the signature of reduced vegetation in response to dry spring/summers with $\delta^{18}O$-enriched precipitation; relatively unchanged $\delta^{18}O$, not biased towards lower $\delta^{18}O$ values, suggests autumn-winter droughts as well. The abrupt transition to dry and cold conditions was followed by gradual recovery of the vegetation cover.

In the broader temporal and spatial context, this potential centennial-scale '7.4 ka event' is an episode within HCO (between 9.5 and 5.5 ka, Lowe and Walker, 2015) which is, in the Eastern Mediterranean, usually coupled with the last Sapropel event (S1), broadly synonymous with a Holocene pluvial phase in Mediterranean (e.g. Filippidi et al., 2016 and references therein). Sapropel events are quasi-periodical occurrences of organic-rich marine sediments formed in an anoxic environments due to the shutdown of local thermohaline circulation responsible for the oxygenation (Vadsaria et al., 2019). Reasons for such conditions are climate-driven surface-water freshening, reduced deep-water ventilation and increased export production (Grant et al., 2016), mainly caused by enhanced rainfall in the Nile River catchment. Combined palynological and geochemical analysis of lake sediment core from eastern Adriatic Vrana Lake provides evidence of climate changes associated with deposition of sapropel S1. Specifically, two sapropelic layers (S1a and S1b, Fig. 7) were identified, separated by a horizon at 7.9-7.4 cal ky BP that corresponds to the drier climate conditions (Bakrač et al., 2018). Similarly, a pluvial period reconstructed from eastern Adriatic former lake (presently sea bay) Malo jezero (Mljet Island) lasted from 8.4 ka to 6 ka, but apparently was interrupted by a drier episode from about 7.2 ka to 7.1 ka (Wunsam et al., 1999). This coincides with the timing of a sudden shift towards drier conditions after the significant wet period at Corchia, as revealed in the Mean Anomaly Index (Regattieri et al., 2014a) (Fig. 7). Based on the combined planktonic and benthic stable oxygen and carbon isotopes from South Adriatic marine core MD 90-917, two main mid-Holocene sea surface temperature (SST) coolings were reported at 8.2 ka and within post-sapropel S1b phase between 7.3 and 6.3 ka (Siani et al., 2013) (Fig. 7). These cooling episodes are related to long-term (multi-decadal) periods of strong winter inflow of cold and dry air from eastern Europe, causing severe northeast winds (*bora*) along the eastern Adriatic coast (Rohling et al., 2002; Siani et al., 2013) which is also the principal mechanism for cool Adriatic deep water (ADW) forming (Checa et al., 2020).

These findings suggest regional hydroclimate instability within the relatively stable HCO. However, it has already been established that rapid climate shifts may have synchronous impact globally, although the effects can be regionally variable or even contrasting (Head, 2019). Thus, around 7.5 ka, while the NG site and southern regions experienced a drier and/or colder episode, some of the eastern European sites recorded warming, e.g. Hungarian Leány Cave from 7 ka to 6 ka (Demény et al., 2013) or Romanian V11 cave from 7.6 ka to 5.6 ka (Tămaş et al., 2005).

Globally, along with the rejection of '7.5-7.0 ka anomaly' as a worldwide multicentennial climate event as proposed by Hou et al. (2019), Holocene climate instability during the 8.0-7.0 ka period was tied to '7.2 ka event' introduced by Feng et al. (2019) (earlier discussed in Wang et al., 2005). According to the multi-proxy speleothem-based reconstruction, it started at 7.29 ± 0.03 ka BP, lasted nearly 200 years and was characterized by the weakening of Asian monsoon (AM) and drought episodes in SW China. Due to the consistency of the speleothem record and Greenland GISP2 ice core $\delta^{18}O$, decreased Pacific and Atlantic SSTs, as well as sunspot activity (i.e. orbitally induced insolation changes), Feng et al. (2019) imply that '7.2 ka event' may have global significance. Either way, the NG record provides evidence of an apparent climate anomaly which could contribute to the eventual establishment of this event on a more widespread scale, some time between 7.0 and 7.5 ka.

The negative phase of the North Atlantic Oscillation (NAO), a major synoptic meteorological feature responsible for European interannual to multi-decadal climate dynamics, (NAO−, low sea-level pressure difference between Azores High and the Icelandic Low; Hurrell, 1995), generates increased storm activity and precipitation amounts in the Mediterranean (Hurrell and Deser, 2010). When considering central, eastern and southern Europe, the most pronounced differences between NAO+ and NAO− precipitation amounts appear to be along the eastern Adriatic coast and Dinarides (see Fig 1. in Perşoiu et al., 2017). Thus, Croatian sites are expected to record significant differences between those two phases. According to Perşoiu et al. (2017) atmospheric circulation patterns similar to NAO− phase prevailed during the early and mid-Holocene in East-Central Europe, while the late Holocene has been characterized with conditions resembling a NAO+ phase. An abrupt transition occurred around 4.7 ka, marking a conversion from the early/mid-Holocene period of generally humid conditions with occasional episodes of intensified seasonality, to the drier period of late Holocene (Perşoiu et al., 2017). Likewise, the end of mid-Holocene NG-3 record is also marked with an abrupt $\delta^{18}O$ increase from $4.67^{+0.47}/_{-0.33}$ ka toward maximum $\delta^{18}O$ values at around 4.2 ka.

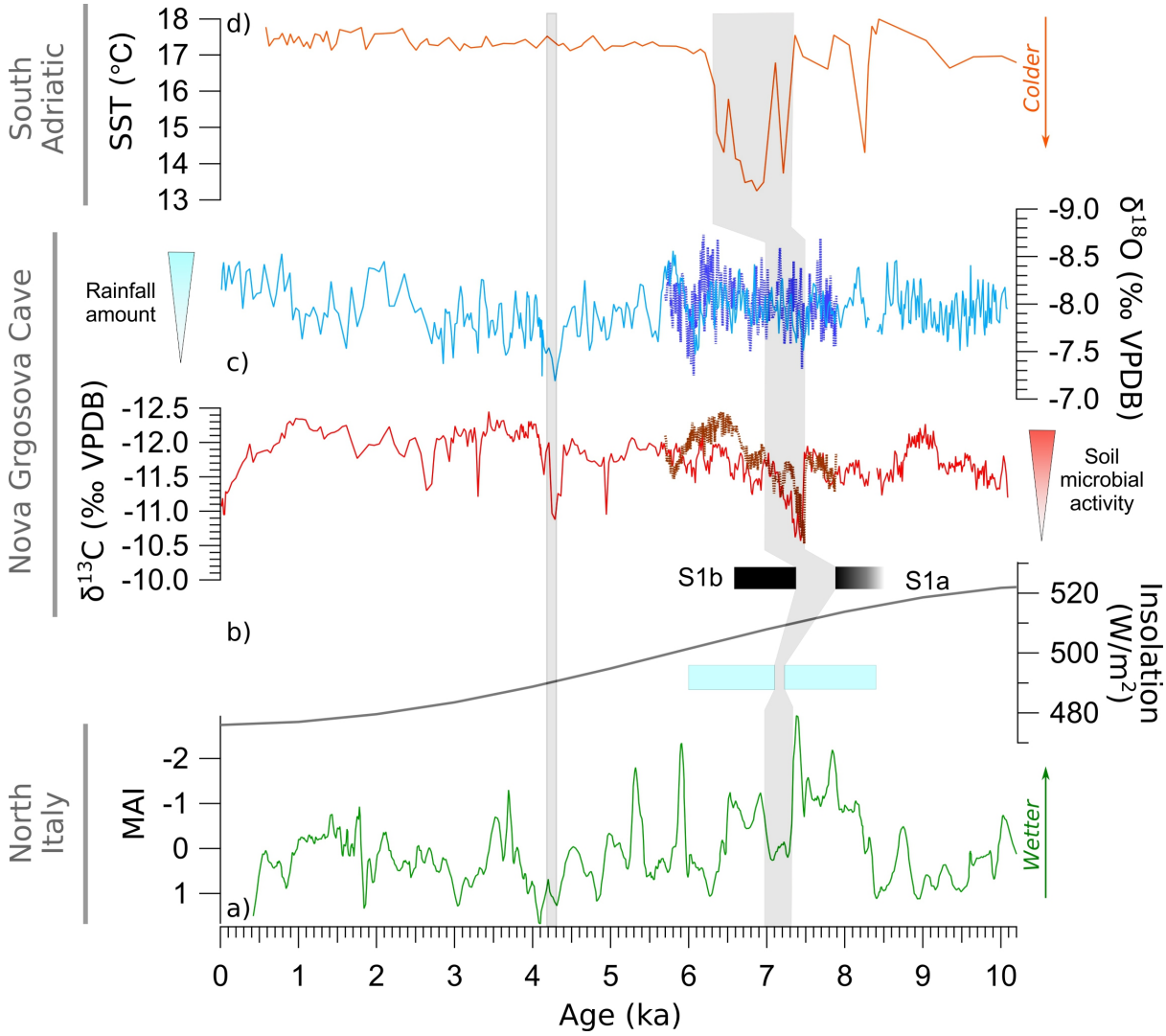

Figure 7 Comparison of NG-3 and NG-7 stalagmites $\delta^{18}O$ and $\delta^{13}C$ time series data (c) with a) Mean Anomaly Index (MAI) derived from Corchia Cave data (Regattieri et al., 2014a; Bajo et al., 2016), b) north hemisphere insolation and d) sea surface temperature (SST) reconstructed from the South Adriatic marine core MD 90-917 (Siani et al., 2013). Black rectangles mark sapropelic layer S1 from Vrana Lake divided into two episodes S1a and S1b (Bakrač et al., 2018) and blue rectangles refers to Malo Jezero Lake (Mljet Island) pluvial phase interrupted from about 7.2 ka to 7.1 ka (Wunsam et al., 1999).

5.4 *Upper (Late) Holocene*

Transition to Megahayalan stage (i.e. Upper/Late Holocene: 4.2 ka to Present) is recorded solely in NG-3 stalagmite and is marked by the highest $\delta^{18}O$ values, increased $\delta^{13}C$ and very slow growth (Fig. 5). It corresponds to the timing of 4.2 ka event, the purportedly global aridification episode caused by deflected monsoon and ocean-atmosphere circulation system that resulted with century-scale precipitation disruptions (Weiss, 2016). The reduction in precipitation delivered by the Mediterranean westerlies in the eastern hemisphere was estimated to be 30-50% (Weiss, 2016) and, according to the thorough overview of the 4.2 ka event in the Mediterranean region by Bini et al. (2019), general hydrological conditions were more arid but with some locally opposed responses. Indeed, temperature decrease was not the common feature in the whole area considered. Speleothem records from the eastern Adriatic insular caves Strašna peć (Dugi otok Island) (Lončar et al., 2019) and Mala špilja (Mljet

Island) (Lončar et al., 2017) both point to dry environmental conditions around 4.2 ka (Fig. 6), as well as some other regional proxies from the cores from Busuja Bay in Istria (Kaniewski et al., 2018), Lake Vrana (Cres Island) (Schmidt et al., 2000) and Bokanjačko blato in North Dalmatia (Ilijanić et al., 2018). Although the climate type of the NG region does not fully correspond to the Mediterranean climate of Bini et al. (2019) (based roughly on the reach of the olive tree), NG speleothem clearly recorded this sudden anomaly. Contrary to the early and mid-Holocene patterns, simultaneous $\delta^{18}O$ and $\delta^{13}C$ increase suggests that precipitation was decreased on annual level, and not only during the spring/summer season. As for the temperature, based on the South Adriatic SST (Siani et al., 2013) in the absence of other temperature indicators, we can tentatively conclude that the MAAT remained stable throughout the 4.2 ka event.

On millennial time scales, the long-term decrease in $\delta^{13}C$ values between 10 and 1 ka BP is probably a consequence of a progressive change in soil-cover thickness, since mature soil contains more organic matter with higher soil pCO_2, which leads to lower $\delta^{13}C$ (Scholz et al., 2012). At the same time, $\delta^{18}O$ slowly increases, suggesting a subtle drying trend. The last thousand years appear stable in terms of precipitation amount and uniform seasonal distribution, as observed also during the instrumental period (Fig. 1), but $\delta^{13}C$ shows a rather conspicuous increase from -12.3‰ to -11.0‰ along with modern farmed calcite having even higher $\delta^{13}C$ values from -9.6‰ to -8.4‰. We might presume that the surface above the cave has been deforested during the last millennium for various human activities, while modern values are additionally increased due to the clearance of the forest and topsoil for the lime production (which eventually led to the NG cave opening in 2004).

5.5 *Possible impact of human (pre)history to speleothem record*

The cave-based research of interrelation between Quaternary environmental changes and human occurrence and further advancement in the Late Quaternary can be successfully complemented by archaeological findings, which are common in Croatia. During the Palaeolithic, human hunter-gatherers used caves as occasional shelters or as more permanent habitats. In continental Croatia, near NG cave, rich archaeological material can be found, such as the world famous Neanderthal site in the cave in Hušnjakovo brdo (40 km NE) (Gorjanović-Kramberger, 1906), Vindija Cave (75 km NE) (Karavanić et al., 2006) and Veternica Cave near Zagreb (15 km E) (Malez, 1979; Banda and Karavanić, 2019), at the time when NG was still a cavern without a natural entrance. By the end of the Early Holocene, Late Palaeolithic and Mesolithic sites in littoral Croatia were inhabited by forager-fishers (Pilaar Birch and Linden, 2018), but their way of life and population distribution were substantially affected and governed by the environmental changes since sea-level fluctuations considerably reshaped the landscape (Pilaar Birch and Miracle, 2017), as reconstructed, for example, in Vela Spila Cave (Korčula Island) site (Dean et al., 2020). Human activities through this period left imprints mainly in clastic cave sediments, but the speleothems were too insensitive to record the overall human impact to the environment. Finally, by the Mid-Holocene, during the first agricultural revolution in the Early Neolithic, deforestation appeared as one of the earliest human impact on the environment (Fairchild and Baker, 2012). Particularly in speleothems, this should leave a palaeoenvironmental signal in form of higher $\delta^{13}C$ values (Jiménez de Cisneros and Caballero, 2011), so the earlier discussed positive $\delta^{13}C$ shift around 7.4 ka in NG stalagmites could be explained by anthropogenic deforestation. However, Neolithisation – a shift from the hunter-gatherer nomadic to sedentary agricultural lifestyle – ushered also permanent settlements often built on the riverbanks (Botić, 2016a). In continental Croatia, Early Neolithic sites were discovered mainly in the eastern part in the lowlands (Botić, 2016b), while the hilly region of NG cave retains no sign of human settlements, supporting hydroclimate causes of isotopic variations,

rather than anthropogenic. In the Slovenian region of Bela Krajina (50 km SW from NG), Andrič (2007) detected beech (*Fagus*) decline from 7.5 to 7.0 ka, but no archaeological site can confirm an anthropogenic cause of this vegetation change. Only archaeobotanical research of Neolithic/Eneolithic sites from around 6.1 ka reveal frequent forest clearance and burning events, most likely human-induced (Andrič, 2007). At the same time, in the aforementioned Vela Spila Cave (Korčula Island), absence of clastic cave sediments from the period of the stabilised vegetation on the slopes was followed by evidence of the Late Neolithic soil erosion interpreted as a consequence of anthropogenic deforestation for agriculture and pastoralism (Dean et al., 2020).

As for the last millennium, historical documents attest to the existence of copper mines from the 13th century near the village of Rude (3 km S from NG cave), while the actual beginning of mining can be traced back to the Roman Period (Vrkljan and Lebegner, 2008). Mining was particularly intensified during the 16th and 17th centuries when copper mines in Rude were some of the largest in Europe (Vrkljan and Lebegner, 2008), so expanding copper production brought numerous miners from across the Europe (Šebečić, 1994). The increasing number of settlers required more arable lands for food production and more timber for housing, mine timber (supporting pillars) and smelting, leading to intensive deforestation, particularly when the size of the mines and their production is considered. In 1784, French naturalist Balthasar Hacquet documented *fuel shortage* which clearly indicates that at the time surrounding forests were already depleted (Grakalić, 2006).

This anthropogenic influence could have masked the potential impact of rapid climate changes such as those of the Medieval Warm Period or Little Ice Age, but at the same time it might have marked the local Holocene–Anthropocene boundary (Waters et al., 2018).

6. Conclusions

The first speleothem $\delta^{13}C$ and $\delta^{18}O$ record from Nova Grgosova Cave in continental Croatia provides insights into Holocene hydroclimate. Several multi-decadal to multi-centennial isotope excursions were climate related, which could be linked to local, regional and global changes, as follows:

- From 9.2 to 8.8 ka BP local environmental conditions improved in terms of vegetation dynamics with consequent increased speleothem growth rate, in spite of regionally decreased temperatures.
- As the 8.2 ka event has not been completely recorded by distinct isotopic shifts, we assume that the site was not water limited during the period of vegetation growth and the main characteristic was a change in the seasonal distribution of precipitation, unlike today. Climate changes associated with temperature variations cannot be observed in the $\delta^{18}O$ of our speleothems.
- Around 7.4 ka, within the Holocene Climate Optimum, an abrupt $\delta^{13}C$ increase points to environmental deterioration, i.e. reduced vegetation and soil microbial activity in response to enhanced spring-summer aridity. Given the minimal $\delta^{18}O$ variability, it appears that the winter-autumn precipitation was also reduced, most probably due to long-term inflow of cold and dry east-European air.
- The 4.2 ka event is marked by an overall short-term precipitation reduction, without significant temperature changes.
- The latest short-term (centennial) climatic variability throughout the last millennium could not be reconstructed due to an apparent human intervention into the natural forest landscape.

Acknowledgements

We are grateful to Grgos family, the concessionaire of the Nova Grgosova Cave and Public Institution *Green Ring of Zagreb County* for the long-term fruitful cooperation. N. Buzjak and S. Buzjak are acknowledged for the field assistance during the cave monitoring. We thank Roman Witt for assistance with the stable isotope analyses and Rieneke Weij for U-Th sampling at The University of Melbourne. We also thank Croatian Meteorological and Hydrological Service for providing climatological and meteorological data. This research was performed within the project *Reconstruction of the Quaternary environment in Croatia using isotope methods* (HRZZ-IP-2013-11-1623) financed by the Croatian Science Foundation.

Literature

Allan M, Deliège A, Verheyden S et al. (2018a) Evidence for solar influence in a Holocene speleothem record (Père Noël cave, SE Belgium). *Quaternary Science Reviews* 192: 249-262.

Allan M, Fagel N, van der Lubbe HJ et al. (2018b) High-resolution reconstruction of 8.2-ka BP event documented in Père Noël cave, southern Belgium. *Journal of Quaternary Science* 33: 840-852.

Andrič M (2007) Holocene vegetation development in Bela krajina (Slovenia) and the impact of first farmers on the landscape. *The Holocene* 17(6): 763-776.

Bajo P, Hellstrom J, Frisia S et al. (2016) "Cryptic" diagenesis and its implications for speleothem geochronologies. *Quaternary Science Reviews* 148: 17-28.

Bajo P, Borsato A, Drysdale R et al. (2017) Stalagmite carbon isotopes and dead carbon proportion (DCP) in a closed system situation: an interplay between sulfuric and carbonic acid dissolution. *Geochimica Cosmochimica Acta* 210: 2018-227.

Bajo P, Drysdale R, Woodhead J et al. (2020) Persistent influence of obliquity on ice age terminations since the Middle Pleistocene transition. *Science* 367: 1235-1239.

Baker A, Barnes W and Smart P (1997) Variations in the discharge and organic matter content of stalagmite drip waters in Lower Cave, Bristol. *Hydrological Processes* 11: 1541-1555.

Bakrač K, Ilijanić N, Miko S et al. (2018) Evidence of sapropel S1 formation from Holocene lacustrine sequences in Lake Vrana in Dalmatia (Croatia). *Quaternary International* 494: 5-18.

Baldini JUL, McDermott F and Fairchild IJ (2006) Spatial variability in cave drip water hydrochemistry: implications for stalagmite paleoclimate records. *Chemical Geology* 235: 390-404.

Baldini LM, Baldini JUL, McDermott F et al. (2019) North Iberian temperature and rainfall seasonality over the Younger Dryas and Holocene. *Quaternary Science Reviews* 226: 105998.

Banda M and Karavanić I (2019) The Mousterian industry of Veternica Cave (in Croatian). *Prilozi Instituta za arheologiju u Zagrebu* 36: 5-40.

Bar-Matthews M and Ayalon A (2011) Mid-Holocene climate variations revealed by high resolution speleothems records from Soreq Cave, Israel and their correlation with cultural changes. *The Holocene* 21: 163-171.

Bar-Matthews M, Ayalon A Kaufman et al. (1999) The Eastern Mediterranean paleoclimate as a reflection of regional events: Soreq cave, Israel. *Earth and Planetary Science Letters* 166 (1-2): 85-95.

Bar-Matthews M, Ayalon A, Gilmour M et al. (2003) Sea-land oxygen isotopic relationships from planktonic foraminifera and speleothems in the Eastern Mediterranean region and

their implication for paleorainfall during interglacial intervals. *Geochimica et Cosmochimica Acta* 67(17): 3181-3199.

Belli R, Frisia S, Borsato A et al. (2013) Regional climate variability and ecosystem responses to the last deglaciation in the northern hemisphere from stable isotope data and calcite fabrics in two northern Adriatic stalagmites. *Quaternary Science Reviews* 72: 146-158.

Berkelhammer M, Sinha A, Stott L et al. (2012) An abrupt shift in the Indian monsoon 4000 years ago. *Geophysical Monograph Series* 198: 75-87.

Bini M, Zanchetta G, Perşoiu A. et al. (2019) The 4.2 ka BP Event in the Mediterranean region: an overview. *Climate of the Past* 15: 555-577.

Boch R, Spötl C and Kramers J. (2009) High-resolution isotope records of early Holocene rapid climate change from two coeval stalagmites of Katerloch Cave, Austria. *Quaternary Science Reviews* 28: 2527-2538.

Boch R, Cheng H, Spötl C et al. (2011) NALPS: a precisely dated European climate record 120–60 ka. *Climate of the Past* 7, 1247-1259.

Bond G, Showers W, Cheseby M et al. (1997) A pervasive millenial-scale cycle in North Atlantic Holocene and glacial climates. *Science* 278: 1257-1266.

Bond G, Kromer B, Beer J et al. (2001) Persistent solar influence on North Atlantic climate during the Holocene. *Science* 294: 2130-2136.

Botić K (2016a) Climatic influences on appearance and development of Neolithic cultures in southern outskirts of Carpathian Basin. *Studia Quaternaria* 33(1): 11-26.

Botić K (2016b) Neolithisation of Sava-Drava-Danube interfluve at the end of the 6600–6000 BC period of Rapid Climate Chang: a new solution to an old problem. *Documenta Praehistorica* 43: 183-208.

Budsky A, Scholz D, Wassenburg JA et al. (2019) Speleothem $\delta^{13}C$ record suggests enhanced spring/summer drought in south-eastern Spain between 9.7 and 7.8 ka – A circum-Western Mediterranean anomaly? *The Holocene* 29(7): 1113-1133.

Checa H, Margaritelli G, Pena LD, et al. (2020) High resolution paleo-environmental changes during the Sapropel 1 in the North Ionian Sea, central Mediterranean. *The Holocene* 30(11): 1504-1515.

Cheng H, Edwards RL, Shen CC et al. (2013) Improvements in ^{230}Th dating, ^{230}Th and ^{234}U half-life values, and U-Th isotopic measurements by multi-collector inductively coupled plasma mass spectrometry. *Earth and Planetary Science Letters* 371-372: 82-91.

CMHS (2020) Croatian Meteorological and Hydrological Service

Collister C and Mattey D (2005) High resolution measurement of water drip rates in caves using an acoustic drip counter. American Geophysical Union Fall Meeting 2005. San Francisco, USA, pp. 31A-1496.

Columbu A, Drysdale R, Capron E et al. (2017) Early last glacial intra-interstadial climate variability recorded in a Sardinian speleothem. *Quaternary Science Reviews* 169: 391-397.

Columbu A, Sauro F, Lundberg J et al. (2018) Palaeoenvironmental changes recorded by speleothems of the southern Alps (Piani Eterni, Belluno, Italy) during four interglacial to glacial climate transitions. *Quaternary Science Reviews* 197: 319-335.

Columbu A, Spötl C, De Waele J et al. (2019) A long record of MIS 7 and MIS 5 climate and environment from a western Mediterranean speleothem (SW Sardinia, Italy). *Quaternary Science Reviews* 220: 230-243.

Columbu A, Chiarini V, Spötl C et al. (2020) Speleothem record attests to stable environmental conditions during Neanderthal-Modern Human turnover in Southern Italy. *Nature Ecology & Evolution* 4: 1188-1195.

Combourieu-Nebout N, Peyron O, Bout-Roumazeilles V et al. (2013) Holocene vegetation and climate changes in the central Mediterranean inferred from a high-resolution marine pollen record (Adriatic Sea). *Climate of the Past* 9: 2023-2042.

Constantin S, Bojar A-V, Lauritzen S-E et al. (2007) Holocene and Late Pleistocene climate in the sub-Mediterranean continental environment: A speleothem record from Poleva Cave (Southern Carpathians, Romania). *Palaeogeography, Palaeoclimatology, Palaeoecology* 243: 322-338.

Corrick EC, Drysdale RN, Hellstrom JC et al. (2020) Synchronous timing of abrupt climate changes during the last glacial period. *Science* 369 (6506): 963-969

Couchoud I, Genty D, Hoffmann D et al. (2009) Millennial-scale climate variability during the Last Interglacial recorded in a speleothem from southwestern France. *Quaternary Science Review* 28: 3263-3274.

Dean S, Pappalardo M, Boschian G et al. (2020) Human adaptation to changing coastal landscapes in the Eastern Adriatic: Evidence from Vela Spila cave, Croatia. *Quaternary Science Reviews* 244: 106503.

Demény A, Czuppon G, Siklósy Z et al. (2013) Mid-Holocene climate conditions and moisture source variations based on stable H, C and O isotope compositions of speleothems in Hungary. *Quaternary International* 293: 150-156.

Demény A, Kern Z, Czuppon G et al. (2019) Middle Bronze Age humidity and temperature variations, and societal changes in East-Central Europe. *Quaternary International* 504: 80-95.

Domínguez-Villar D, Wang X, Cheng H et al. (2008). A high-resolution late Holocene speleothem record from Kaite Cave, northern Spain: $\delta^{18}O$ variability and possible causes. *Quaternary International* 187(1): 40-51.

Domínguez-Villar D, Fairchild IJ, Baker A et al. (2009) Oxygen isotope precipitation anomaly in the North Atlantic region during the 8.2 ka event. *Geology* 37: 1095-1098.

Domínguez-Villar D, Wang X, Krklec K et al. (2017) The control of the tropical North Atlantic on Holocene millennial climate oscillations. *Geology* 45(4): 303-306.

Domínguez-Villar D, Lojen S, Krklec K et al. (2018) Ion microprobe $\delta^{18}O$ analyses to calibrate slow growth rate speleothem records with regional $\delta^{18}O$ records of precipitation. *Earth and Planetary Science Letters* 482: 367-376.

Dorale JA and Liu Z (2009) Limitations of Hendy Test criteria in judging the paleoclimatic suitability of speleothems and the need for replication. *Journal of Cave and Karst Studies* 71: 73-80.

Drăguşin V, Staubwasser M, Hoffmann DL et al. (2014) Constraining Holocene hydrological changes in the Carpathian–Balkan region using speleothem $\delta^{18}O$ and pollen-based temperature reconstructions. *Climate of the Past* 10: 1363-1380.

Drysdale RN, Zanchetta G, Hellstrom JC et al. (2004) Palaeoclimatic implications of the growth history and stable isotope ($\delta^{18}O$ and $\delta^{13}C$) geochemistry of a Middle to Late Pleistocene stalagmite from central-western Italy. *Earth and Planetary Science Letters* 227(3-4): 215-229.

Drysdale RN, Hellstrom JC, Zanchetta G et al. (2009) Evidence for obliquity forcing of glacial termination II. *Science* 325(5947): 1527-1531.

Fairchild IJ, Borsato A, Tooth AF et al. (2000) Controls on trace element (Sr-Mg) compositions of carbonate cave waters: implications for speleothem climatic records. *Chemical Geology* 166(3-4): 255-269.

Fairchild IJ and Baker A (2012) *Speleothem Science: From Process to Past Environments*. Chichester: Wiley-Blackwell.

Feng X, Yang Y, Cheng H et al. (2020) The 7.2 ka climate event: Evidence from high-resolution stable isotopes and trace element records of stalagmite in Shuiming Cave, Chongqing, China. *The Holocene* 30(1):145-154.

Filippidi A, Triantaphyllou MV and De Lange GJ (2016) Eastern-Mediterranean ventilation variability during sapropel S1 formation, evaluated at two sites influenced by deep-water formation from Adriatic and Aegean Seas. *Quaternary Science Reviews* 144: 95-106.

Finné M, Bar-Matthews M, Holmgren K et al. (2014) Speleothem evidence for late Holocene climate variability and floods in Southern Greece. *Quaternary Research* 81(02), 213-227.

Finné M, Holmgren K, Shen C-C et al. (2017) Late Bronze Age climate change and the destruction of the Mycenaean Palace of Nestor at Pylos. *PLoS ONE* 12: e0189447.

Fleitmann D, Mudelsee M, Burns SJ et al. (2008) Evidence for a widespread climatic anomaly at around 9.2 ka before present. *Paleoceanography* 23: PA1102

Fleitmann D, Cheng H, Badertscher S et al. (2009) Timing and climatic impact of Greenland interstadials recorded in stalagmites from northern Turkey. *Geophysical Research Letters* 36: L19707.

Fohlmeister J, Vollweiler N, Spötl C et al. (2012a). COMNISPA II: Update of a mid-European isotope climate record, 11 ka to present. *The Holocene* 23(5): 749–754.

Fohlmeister J, Schröder-Ritzrau A, Scholz D et al. (2012b) Bunker Cave stalagmites: an archive for central European Holocene climate variability. *Climate of the Past* 8, 1751-1764.

Frisia S, Borsato A, Spötl C et al. (2005) Climate variability in the SE Alps of Italy over the past 17000 years reconstructed from a stalagmite record. *Boreas* 34(4): 445-455.

Genty D, Blamart D, Ouahdi R et al. (2003) Precise dating of Dansgaard–Oeschger climate oscillations in western Europe from stalagmite data. *Nature* 421(6925): 833-837.

Genty D, Blamart D, Ghaleb B et al. (2006) Timing and dynamics of the last deglaciation from European and North African $\delta^{13}C$ stalagmite profiles – comparison with Chinese and South Hemisphere stalagmites. *Quaternary Science Reviews* 25(17-18): 2118-2142.

Göktürk OM, Fleitmann D, Badertscher S et al. (2011) Climate on the southern Black Sea coast during the Holocene: Implications from the Sofular Cave record. *Quaternary Science Reviews* 30(19-20): 2433-2445.

Gorjanović-Kramberger D (1906) *Der diluviale Mensch von Krapina in Kroatien: Ein beitrag zur Paläoanthropologie, Studien uber die Entwicklungsmechanik des Primatenskelletes*, Wiesbaden: C. W. Kreidie Verlag.

Grakalić D (2006) Rude – stoljetni centar rudarstva. (Rude – centuries-old mining center). *Meridijani* 101: 39-53 (in Croatian)

Grant KM, Grimm R, Mikolajewicz U et al. (2016) The timing of Mediterranean sapropel deposition relative to insolation, sea-level and African monsoon changes. *Quaternary Science Reviews* 140: 125–141.

Head MJ (2019) Formal subdivision of the Quaternary System/Period: Present status and future directions. *Quaternary International* 500: 32-51.

Hellstrom J (2003). Rapid and accurate U/Th dating using parallel ion-counting multi-collector ICP-MS. *Journal of Analytical Atomic Spectrometry* 18: 1346-1351.

Hellstrom JC (2006) U-Th dating of speleothems with high initial ^{230}Th using stratigraphical constraint. *Quaternary Geochronology* 1: 289-295.

Hendy CH (1971) The isotopic geochemistry of speleothems-I: The calculations of the effects of different modes of formation on the isotopic composition of speleothems and their applicability as paleoclimate indicators. *Geochimica et Cosmochimica Acta* 35: 801-824.

Hou M, Wu W, Cohen DJ et al. (2019) Evidence for a widespread climatic anomaly at around 7.5-7.0 cal ka BP. *Climate of the Past Discussion*, https://doi.org/10.5194/cp-2019-89.

Hurrell JW (1995) Decadal trends in the North Atlantic Oscillation: regional temperatures and precipitation. *Science* 269: 676-679.

Hurrell JW and Deser C (2010) North Atlantic climate variability: the role of the North Atlantic Oscillation. *Journal of Marine Systems* 79: 231-244.

Ilijanić N, Miko S, Hasan O. et al. (2018) Holocene environmental record from lake sediments in the Bokanjačko blato karst polje (Dalmatia, Croatia). *Quaternary International* 494: 66-79.

Isola I, Zanchetta G, Drysdale RN et al. (2019) The 4.2 ka event in the central Mediterranean: new data from a Corchia speleothem (Apuan Alps, central Italy). *Climate of the Past* 15: 135-151.

Jiménez de Cisneros, C and Caballero E (2011) Carbon isotope values as paleoclimatic indicators. Study on stalagmite from Nerja Cave, South Spain. *Carbonates Evaporites* 26: 41-46.

Kacanski A, Carmi I, Shemesh A et al. (2001) Late Holocene Climatic Change in the Balkans: Speleothem Isotopic Data from Serbia. *Radiocarbon* 43(2B): 647-658.

Kaniewski D, Marriner N, Morhange C et al. (2018) Croatia's mid-Late Holocene (5200-3200 BP) coastal vegetation shaped by human societies. *Quaternary Science Reviews* 200: 334-350.

Karavanić I, Vukosavljević N, Šošić R et al. (2006) Approaches to the middle Paleolithic rockshelter and cave research in Croatia. In: Kornfeld M, Vasil'ev S and Miotti L (eds) *On Shelter's Ledge: Histories, Theories and Methods of Rockshelter Research,* Proceedings of the XV World Congress, Lisbon, 4-9 September, International Union for Prehistoric and Protohistoric. pp13-22

Kim ST and O'Neil JR (1997) Equilibrium and nonequilibrium oxygen isotope effects in synthetic carbonates. *Geochimica et Cosmochimica Acta* 61: 3461-3475.

Koltai G, Spötl C, Shen C-C et al. (2017) A penultimate glacial climate record from southern Hungary. *Journal of Quaternary Science* 32: 946-956.

Krajcar Bronić I, Barešić J, Borković D et al. (2020) Long-Term Isotope Records of Precipitation in Zagreb, Croatia. *Water* 12, 226.

Lajeunesse P and St-Onge G (2008) The subglacial origin of the Lake Agassiz– Ojibway final outburst flood. *Nature Geoscience* 1: 184–188.

Lechleitner F, Amirnezhad-Mozhdehi S, Columbu A et al. (2018) The Potential of Speleothems from Western Europe as Recorders of Regional Climate: a Critical Assessment of the SISAL Database. *Quaternary* 1: 1-31.

Lončar N, Bar-Matthews M, Avalon A et al. (2017) Early and mid-Holocene environmental conditions in the eastern Adriatic recorded in speleothems from Mala špilja Cave and Velika špilja Cave (Mljet Island, Croatia). *Acta Carsologica* 46 (2-3): 229–249.

Lončar N, Bar-Matthews M, Ayalon A et al. (2019) Holocene climatic conditions in the eastern Adriatic recorded in stalagmites from Strašna peć Cave (Croatia). *Quaternary International* 508: 98-106.

Lowe JJ and Walker MJC (2015) *Reconstructing Quaternary Environments,* 3rd ed. London: Routledge.

Lüetscher M, Boch R, Sodemann H et al. (2015) North Atlantic storm track changes during the Last Glacial Maximum recorded by Alpine speleothems. *Nature Communications* 6: 6334.

Mangini A, Spötl C and Verdes P (2005) Reconstruction of temperature in the Central Alps during the past 2000 yr from a $\delta^{18}O$ stalagmite record. *Earth and Planetary Science Letters* 235(3-4): 741-751.

Mangini A, Verdes P, Spötl C et al. (2007) Persistent influence of the North Atlantic hydrography on Central European winter temperature during the last 9000 years. *Geophysical Research Letters* 34: 2704, L02704.

Malez M (1979) Basic features of the Paleolithic and Mesolithic in Croatia (in Croatian). *Rad Jugoslavenske akademije znanosti i umjetnosti* 383: 117-153.

Mayewski PA, Rohling EE, Stager JC et al. (2004) Holocene climate variability. *Quaternary Research* 62(3): 243-255.

McCabe GJ and Markstrom SL (2007) A monthly water-balance driven by a graphical user interface. USGS Open-File report 2007-1088.

McDermott F (2004) Paleo-climate reconstruction from stable isotope variations in speleothems: a review. *Quaternary Science Reviews* 23: 901-918.

McDermott F, Mattey C and Hawkesworth C (2001) Centennial-Scale Holocene Climate Variability Revealed by a High-Resolution Speleothem $\delta^{18}O$ Record from SW Ireland. *Science* 294(5545): 1328–1331.

McDermott F, Atkinson TC, Fairchild IJ et al. (2011) A first evaluation of the spatial gradients in $\delta^{18}O$ recorded by European Holocene speleothems. *Global and Planetary Change* 79(3-4): 275-287.

Mehterian S, Pourmand A, Sharifi A et al. (2017) Speleothem records of glacial/interglacial climate from Iran forewarn of future Water Availability in the interior of the Middle East. *Quaternary Science Reviews* 164: 187-198.

Mickler PJ, Banner JL, Stern L et al. (2004) Stable isotope variations in modern tropical speleothems: Evaluating equilibrium vs. kinetic isotope effects. *Geochimica et Cosmochimica Acta* 68: 4381-4393.

Mischel SA, Scholz D, Spötl C et al. (2017) Holocene climate variability in Central Germany and a potential link to the polar North Atlantic: A replicated record from three coeval speleothems. *The Holocene* 27(4): 509-525.

Moreno A, Pérez-Mejías C, Bartolomé C et al. (2017) New speleothem data from Molinos and Ejulve caves reveal Holocene hydrological variability in northeast Iberia. *Quaternary Research* 88; 223-233.

Moseley GE, Spötl C, Cheng H et al. (2015) Termination-II interstadial/stadial climate change recorded in two stalagmites from the north European Alps. *Quaternary Science Reviews* 127: 229-239.

Moseley GE, Spötl C, Brandstätter S et al. (2020) NALPS19: sub-orbital-scale climate variability recorded in northern Alpine speleothems during the last glacial period. *Climate of the Past* 16: 29-50.

NGRIP, North Greenland Ice Core Project Members (2004) High-resolution record of Northern Hemisphere climate extending into the last interglacial period. *Nature* 431: 147-151.

Niggemann S, Mangini A, Mudelsee M et al. (2003) Sub-Milankovitch climatic cycles in Holocene stalagmites from Sauerland, Germany. *Earth and Planetary Science Letters* 216: 539-547.

Onac BP, Constantin S, Lundberg J et al. (2002) Isotopic climate record in a Holocene stalagmite from Ursilor Cave (Romania). *Journal of Quaternary Science* 17: 319-327.

Perșoiu A, Onac BP, Wynn JG et al. (2017) Holocene winter climate variability in Central and Eastern Europe. *Scientific Reports* 7: 1196.

Pilaar Birch SE and Miracle PT (2017) Human Response to Climate Change in the Northern Adriatic During the Late Pleistocene and Early Holocene. In: Monks G (ed) *Climate Change and Human Responses. Vertebrate Paleobiology and Paleoanthropology*. Dordrecht: Springer.

Pilaar Birch SE and Linden MV (2018) A long hard road… Reviewing the evidence for environmental change and population history in the eastern Adriatic and western Balkans during the Late Pleistocene and Early Holocene. *Quaternary International* 465(B): 177-191.

Psomiadis D, Dotsika E, Albanakis K et al. (2018) Speleothem record of climatic changes in the northern Aegean region (Greece) from the Bronze Age to the collapse of the Roman Empire. *Palaeogeography, Palaeoclimatology, Palaeoecology* 489: 272-283.

Regattieri E, Zanchetta G, Drysdale RN et al. (2014a) Lateglacial to Holocene trace element record (Ba, Mg, Sr) from Corchia Cave (Apuan Alps, central Italy): paleoenvironmental implications. Journal of Quaternary Science 29: 381-392.

Regattieri E, Zanchetta G, Drysdale RN et al. (2014b) A continuous stable isotope record from the penultimate glacial maximum to the Last Interglacial (159-121 ka) from Tana Che Urla cave (Apuan Alps, central Italy). *Quaternary Research* 82(2): 450-461.

Regattieri E, Zanchetta G, Isola I et al. (2018) A MIS 9/MIS 8 speleothem record of hydrological variability from Macedonia (F.Y.R.O.M.). *Global and Planetary Change* 162: 39-52.

Regattieri E, Zanchetta G, Isola I et al. (2019) Holocene Critical Zone dynamics in an Alpine catchment inferred from a speleothem multiproxy record: disentangling climate and human influences. *Scientific Reports* 9: 17829

Rohling EJ, Mayewski PA, Abu-Zied RH et al. (2002) Holocene atmosphere-ocean interactions: Records from Greenland and the Aegean Sea, *Climate Dynamics* 18: 587-593.

Rossi C, Bajo P, Lozano RP et al. (2018) Younger Dryas to Early Holocene paleoclimate in Cantabria (N Spain): Constraints from speleothem Mg, annual fluorescence banding and stable isotope records. *Quaternary Science Reviews* 192: 71-85.

Rozanski K, Sonntag C and Munnich KO (1982) Factors controlling stable isotope composition of European precipitation. *Tellus* 34: 142-150.

Rozanski K, Araguás-Araguás L and Gonfiantini R (1993) Isotopic patterns in modern precipitation. In: Swart PK, Lohmann KC, McKenzie J et al. (eds.) *Climate Change in Continental Isotopic Records*. Geophysical Monograph, 78. American Geophysical Union, Washington, D.C, pp. 1–36.

Rudzka D, McDermott F and Surić M (2012) A late-Holocene climate record in stalagmites from Modrič Cave (Croatia). *Journal of Quaternary Science* 27: 585-596.

Schmidt R, Müller J, Drescher-Schneider R, et al. (2000) Changes in lake level and trophy at Lake Vrana, a large karstic lake on the Island of Cres (Croatia), with respect to palaeoclimate and anthropogenic impacts during the last approx. 16,000 years. *Journal of Limnology* 59(2), 113-130.

Scholz D, Frisia S, Borsato A et al. (2012) Holocene climate variability in north-eastern Italy: potential influence of the NAO and solar activity recorded by speleothem data. *Climate of the Past* 8: 1367-1383.

Scholz D, Hoffmann D, Spötl C et al. (2019) Speleothem record from western Germany suggests a relatively late timing (124-114 ka) of the Last Interglacial in Central Europe. 20th Congress of the International Union for Quaternary Research (INQUA)

Siani G, Magny M, Paterne M et al. (2013) Paleohydrology reconstruction and Holocene climate variability in the South Adriatic Sea. *Climate of the Past* 9: 499-515.

Siklósy Z, Demény A, Vennemann TW et al. (2009) Bronze Age volcanic event recorded in stalagmites by combined isotope and trace element studies. *Rapid Communications in Mass Spectrometry* 23: 801-808.

Smart PL and Friedrich H (1987) Water movement and storage in the unsaturated zone of a maturely karstified aquifer, Mendip Hills, England. Proceedings of the Conference on

Environmental Problems in Karst Terrains and their Solution. National Water Well Association, Bowling Green, Kentucky, pp. 57-87.
Spötl C, Mangini A, Frank N et al. (2002) Start of the last interglacial period at 135 ka: evidence from a high Alpine speleothem. *Geology* 30(9): 815-818.
Spötl C, Mangini A and Richards DA (2006) Chronology and paleoenvironment of marine isotope stage 3 from two high-elevation speleothems, Austrian Alps. *Quaternary Science Reviews* 25(9-10): 1127-1136.
Spötl C, Scholz D and Mangini A (2008) A terrestrial U/Th-dated stable isotope record of the Penultimate Interglacial. *Earth and Planetary Science Letters* 276 (3-4): 283-292.
Stoykova D, Shopov Y, Sauro U et al. (2003) High-Resolution Climate Proxy Records for the Last 2000 Years from a Speleothem from Savi Cave, Trieste, NE Italy. *Studi trentini di scienze naturali. Acta Geologica* 80: 169-173.
Surić M, Lončarić R, Bočić N et al. (2018) Monitoring of selected caves as a prerequisite for the speleothem-based reconstruction of the Quaternary environment in Croatia. *Quaternary International* 494: 263-274.
Surić M (2018) Speleothem-based Quaternary research in Croatian karst – an overview. *Quaternary International* 490: 113-122.
Surić M, Czuppon G, Lončarić R et al. (2020) Stable Isotope Hydrology of Cave Groundwater and Its Relevance for Speleothem-Based Paleoenvironmental Reconstruction in Croatia. *Water* 12(9), 2386.
Šebečić B (1994) Potomci rudara iz XVII. Stoljeća iz Ruda kod Samobora u Hrvatskoj (The offsprings of the 17th-century miners from the village of Rude near Samobor). *Rudarsko-geološko-naftni zbornik* 6: 151-158 (in Croatian).
Šikić K, Basch O and Šimunić A (1978) Osnovna geološka karta SFRJ 1:100 000. List Zagreb. (Basic Geological Map of 1:100,000. Zagreb sheet L 33-80). Savezni geološki zavod, Beograd.
Šikić K, Basch O and Šimunić A (1979) Explanatory notes for the Basic Geological Map 1:100000. Zagreb sheet L 33-80 – in Croatian. Savezni geološki zavod, Beograd.
Tămaş T, Onac BP and Bojar AV (2005) Lateglacial-Middle Holocene stable isotope records in two coeval stalagmites from the Bihor Mountains, NW Romania, *Geological Quarterly* 49: 185-194.
Thatcher DL, Wanamaker AD, Denniston RF et al. (2020) Hydroclimate variability from western Iberia (Portugal) during the Holocene: Insights from a composite stalagmite isotope record. *The Holocene* 30(7): 966-981.
Thornthwaite CW (1948) An approach toward a rational classification of climate. *Geographical Review* 38: 55-94.
Tremaine DM, Froelich PN and Wang Y (2011) Speleothem calcite farmed in situ: Modern calibration of $\delta^{18}O$ and $\delta^{13}C$ paleoclimate proxies in a continuously-monitored natural cave system. *Geochimica et Cosmochimica Acta* 75: 4929-4950.
Trigo IF, Bigg GR and Davies TD (2002) Climatology of cyclogenesis mechanisms in the Mediterranean. *Monthly Weather Review* 130: 549-569.
Ünal-İmer E, Shulmeister J, Zhao J-X et al. (2015) An 80 kyr-long continuous speleothem record from Dim Cave, SW Turkey with paleoclimatic implications for the Eastern Mediterranean. *Scientific Reports* 5: 13560.
Vadsaria T, Ramstein G, Dutay J-C et al. (2019) Simulating the occurrence of the last sapropel event (S1): Mediterranean basin ocean dynamics simulations using Nd isotopic composition modeling. *Paleoceanography and Paleoclimatology* 34: 237-251.
Verheyden S, Keppens E, van Strydonck M et al. (2012) The 8.2 ka event: Is it registered in Belgian speleothems? *Speleogenesis and Evolution of Karst Aquifers* 12: 3-8.

Vrkljan D and Lebegner J (2008) Uređenje starog rudnika željeza u Rudama kraj Samobora (Renovating old iron mine in Rude near Samobor). *Mineral* 12(2): 22-24 (in Croatian)

Vrsaljko D, Pavelić D and Bajraktarević Z (2005) Stratigraphy and palaeogeography of Miocene deposits from the marginal area of Žumberak Mt. and the Samoborsko Gorje Mts. (Northwestern Croatia). *Geologia Croatica* 58(2): 133-150.

Walker M, Head MJ, Berkelhammer M et al. (2018) Formal ratification of the subdivision of the Holocene Series/Epoch (Quaternary System/Period): two new Global Boundary Stratotype Sections and Points (GSSPs) and three new stages/subseries. *Episodes* 41, 213-223.

Wang YJ, Cheng H, Edwards RL et al. (2005) The Holocene Asian monsoon: Links to solar changes and North Atlantic climate. *Science* 308(5723): 854–857.

Wanner H, Solomina O, Grosjean M et al. (2011) Structure and origin of Holocene cold events. Quaternary Science Reviews 30: 3109-3123.

Waters CN, Zalasiewicz J, Summerhayes C et al. (2018) Global Boundary Stratotype Section and Point (GSSP) for the Anthropocene Series: Where and how to look for potential candidates. *Earth-Science Reviews* 178: 379–429.

Weiss H (2016) Global megadrought, societal collapse and resilience at 4.2-3.9 ka BP across the Mediterranean and west Asia. *Past Global Change Magazine* 24(2): 62-63.

White WB (1999) Conceptual models for karstic aquifers. In: Palmer AN, Palmer MV and Sasowsky ID (eds.), *Karst Modeling: Special Publication* 5. Karst Waters Institute Special Publication, The Karst Waters Institute, Charles Town, USA, pp. 11-16.

Wunsam S, Schmidt R and Müller J (1999) Holocene lake development of two Dalmatian lagoons (Malo and Veliko Jezero, Isle of Mljet) in respect to changes in Adriatic Sea level and climate. *Palaeogeography, Palaeoclimatology, Palaeoecology* 146(1-4): 251-281.

Wurth G, Niggemann S, Richter DK et al. (2004) The Younger Dryas and Holocene climate record of a stalagmite from Hölloch Cave (Bavarian Alps, Germany). *Journal of Quaternary Science* 19: 291-298.

Zanchetta G, Drysdale RN, Hellstrom JC et al. (2007) Enhanced rainfall in the Western Mediterranean during deposition of sapropel S1: stalagmite evidence from Corchia cave (Central Italy). *Quaternary Science Reviews* 26: 279-286.

Zanchetta G, Bar-Matthews M, Drysdale RN et al. (2014) Coeval dry events in the central and eastern Mediterranean basin at 5.2 and 5.6 ka recorded in Corchia (Italy) and Soreq caves (Israel) speleothems. *Global and Planetary Change* 122: 130-139.

Zhornyak LV, Zanchetta G, Drysdale RN et al. (2011) Stratigraphic evidence for a "pluvial phase" between ca. 8200-7100 ka from Renella Cave (Central Italy). *Quaternary Science Reviews* 30: 409-417.

Supplement material

Assessment of equilibrium calcite precipitation

An assessment of whether calcite is deposited at or near isotopic equilibrium with drip water is key prerequisite for reliable interpretation of spelean $\delta^{18}O$ and $\delta^{13}C$. Kinetic processes, such as fast CO_2 degassing or evaporation, can modify the environmental signal (Hendy, 1971, McDermott, 2004). To estimate near-equilibrium fractionation during NG speleothem precipitation, we employed three different approaches: i) the traditional but recently contested Hendy test based on correlation and range of $\delta^{18}O$ and $\delta^{13}C$ values along single layers (Hendy, 1971); ii) the replication test, which requires simultaneous temporal variations of $\delta^{18}O$ and/or $\delta^{13}C$ in at least two coeval speleothems (Dorale and Liu, 2009); and iii) an evaluation of equilibrium fractionation of modern calcite with known modern $\delta^{18}O$ of the calcite ($\delta^{18}O_c$), drip water ($\delta^{18}O_w$) and cave temperature.

For the Hendy test, 6 laminae from each speleothem were examined, with a total of 69 samples. A lack of correlation between $\delta^{18}O$ and $\delta^{13}C$ is evident in all examined layers (Figs. S1 and S2), except for the NG-3_TIV and NG-7_TV which returned a correlation coefficient of r = 0.8 and r = 0.9, respectively. However, non-correlation in Hendy tests is not an absolute proof of equilibrium deposition since the $\delta^{18}O$ and $\delta^{13}C$ may covary simply because of a coupled response to climate drivers (Dorale and Liu, 2009). Additionally, in the case of temperature-dependent oxygen isotope fractionation without kinetic effects, $\delta^{18}O$ is supposed to keep near-constant values along single layers (Lauritzen and Lundberg, 1999) as demonstrated in Fig. S3. There was no significant isotopic enrichment away from central axes and the largest $\delta^{18}O$ difference in single layer was 0.38‰ which is below the threshold value of 0.8‰ determined by Gascoyne (1992).

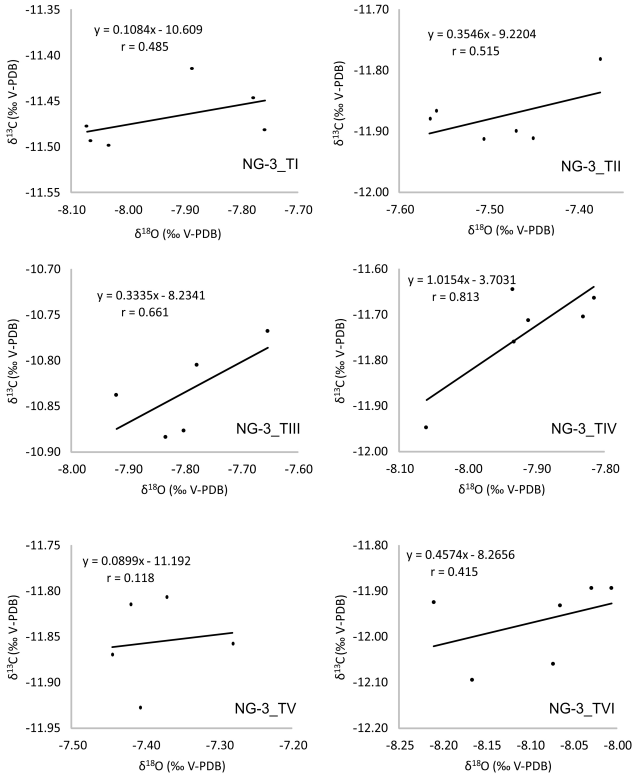

Figure S1 Correlation between $\delta^{18}O$ and $\delta^{13}C$ values along the single laminae of NG-3 stalagmite. Graph titles relates to the yellow lines in Fig. 4 in the main text.

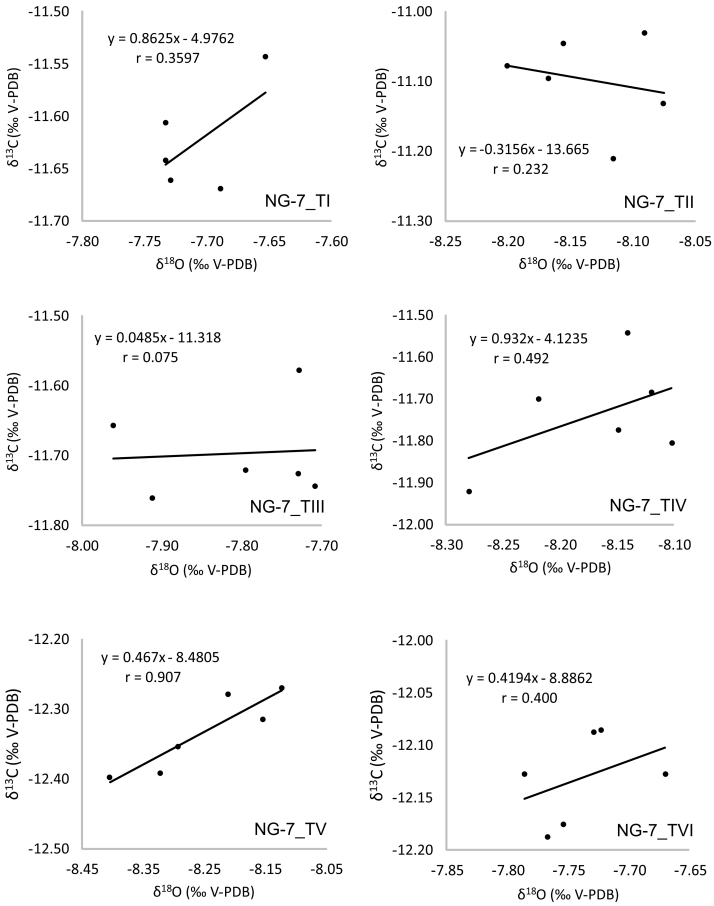

Figure S2 Correlation between $\delta^{18}O$ and $\delta^{13}C$ values along the single laminae of NG-7 stalagmite. Graph titles relates to the yellow lines in Fig. 4 in the main text.

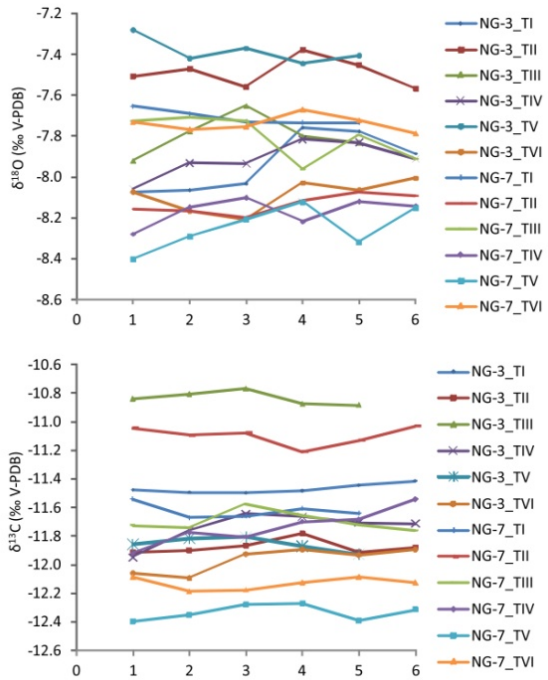

Figure S3 $\delta^{18}O$ and $\delta^{13}C$ values along single layers of NG-3 and NG-7 speleothems. Series names relate to the yellow lines in Fig. 4 of the main text.

Another indicator of near-equilibrium deposition evident in NG speleothems is coherence between isotopic profiles i.e. simultaneous variations of $\delta^{18}O$ and $\delta^{13}C$ values during the period of their concurrent growth from 7.9 ka to 5.7 ka (Fig. S4). Such resemblance under kinetic fractionation is hardly possible since it would require equal response of both speleothems to dynamic processes (Dorale and Liu, 2009). More probable is simply the absence of kinetic effect.

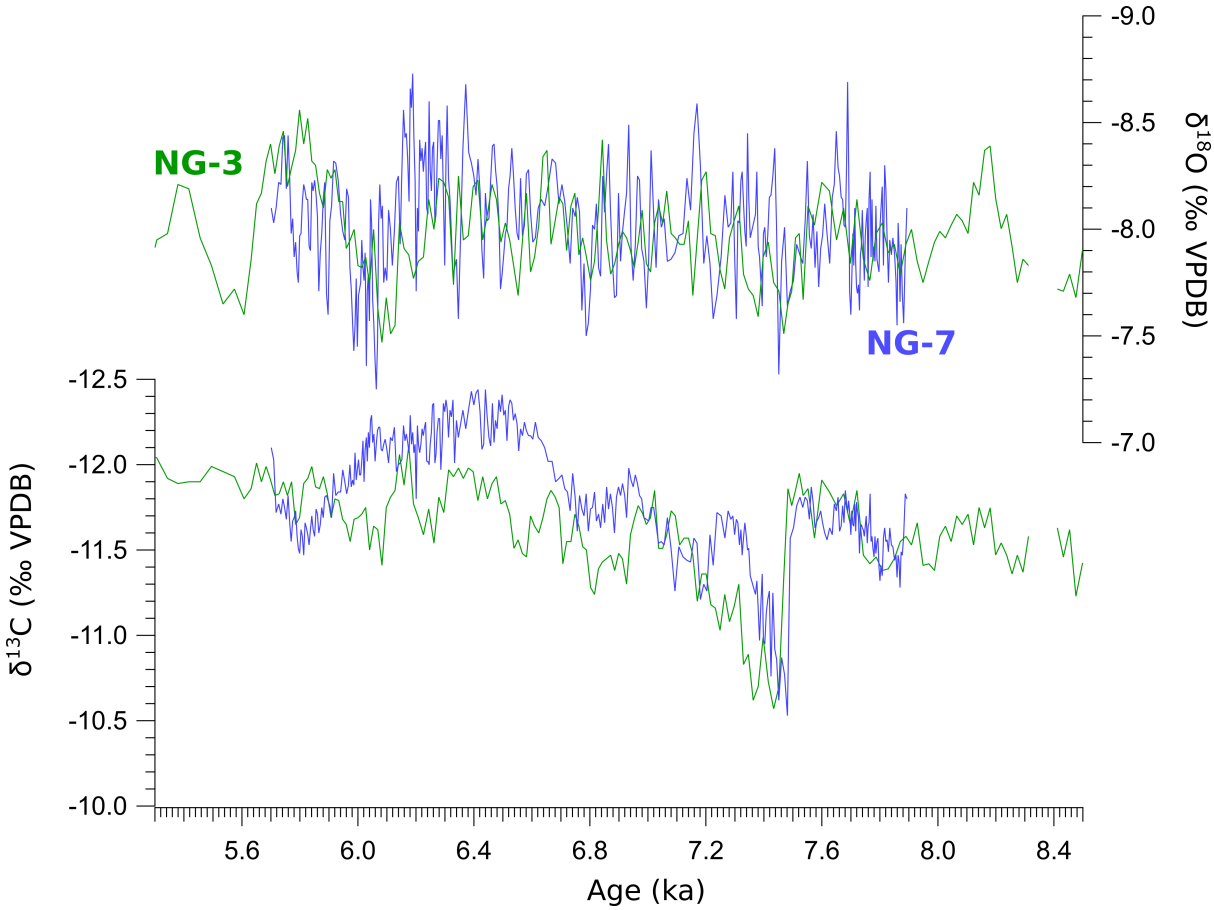

Figure S4 Replication of NG-3 and NG-7 stable isotope record during the concurrent growth from 7.9 ka to 5.7 ka

Additional test that could confirm near-equilibrium conditions takes into account oxygen values of the modern calcite ($\delta^{18}O_C$) and dripwater ($\delta^{18}O_W$) in order to compare measured (T_m) temperature and those calculated (T_c) after the empirical relationships for water–calcite oxygen isotope fractionation. We used equation $1000 \ln \alpha = 16.1(10^3 T^{-1}) - 24.6$ proposed by Tremaine et al. (2011), where $\alpha = (1000+ \delta^{18}O_C)/(1000+ \delta^{18}O_W)$. As the modern calcite has not been farmed on the glass plate at the NG-3 position, we used the youngest $\delta^{18}O_C$ value from the axial stable isotope series that is -8.15‰ (V-PDB), given the fact that NG-3 stalagmite has been actively growing at the moment of the collection. Mean $\delta^{18}O_W$ for the period from Nov 2014 to Oct 2015 was -9.8 ± 0.09‰ (V-SMOW), and mean cave T_m for the same period was 11.2 °C which is close to the calculated value T_c= 10.8 ± 0.4°C.

Given the stable cave atmosphere with constant air temperature and relative humidity close to 100%, and very good homogenization of the dripwater without seasonal variations, these three sources of evidence of near-equilibrium deposition give us confidence that the isotopic signals recorded in the spelean calcite truly presents palaeoenvironmental changes above Nova Grgosova Cave.

Literature

Dorale JA and Liu Z (2009) Limitations of Hendy Test criteria in judging the paleoclimatic suitability of speleothems and the need for replication. *Journal of Cave and Karst Studies* 71: 73-80.

Gascoyne M (1992) Paleoclimate determination from cave calcite deposits. *Quaternary Science Reviews* 11: 609-632.

Hendy CH (1971) The isotopic geochemistry of speleothems-I: The calculations of the effects of different modes of formation on the isotopic composition of speleothems and their applicability as paleoclimate indicators. *Geochimica et Cosmochimica Acta* 35: 801-824.

Lauritzen S-E and Lundberg J (1999) Calibration of the speleothem delta function: an absolute temperature record for the Holocene in northern Norway. *The Holocene* 9(6): 659-669.

McDermott F (2004) Paleo-climate reconstruction from stable isotope variations in speleothems: a review. *Quaternary Science Reviews* 23: 901-918.

Tremaine DM, Froelich PN and Wang Y (2011) Speleothem calcite farmed in situ: Modern calibration of $\delta^{18}O$ and $\delta^{13}C$ paleoclimate proxies in a continuously-monitored natural cave system. *Geochimica et Cosmochimica Acta* 75: 4929-4950.